March 2016

Analysis of 3d Printed Beams and Truss Bridges

Aaron William Cornelius
Worcester Polytechnic Institute

Analysis of 3d Printed Beams and Truss Bridges

A Major Qualifying Project
Submitted to the faculty of
WORCESTER POLYTECHNIC INSTITUTE
In partial fulfillment of the requirements for the
Degree in Bachelor of Science
By:

Aaron Cornelius

Submitted on March 6th, 2015

Project Advisor: Torbjorn Bergstrom, WPI Mechanical Engineering

Abstract

Fused Deposition Modeling (FDM), a common form of 3d printing, has several key drawbacks that make it difficult to analyze using traditional engineering equations. This paper analyzed traditional engineering models in regards to 3d printed beams in bending and proposes adapted equations. The proposed infill based model accurately predicts the failure point of beams, and is suitable for both direct calculation of beam strength and for comparative analysis with changing part dimensions and printing variables. Additionally, a new system for breaking 3d printed truss bridges is proposed for use in educational settings, which allows quick and simple setup with minimal printing time.

Table of Contents

Table of Figures

Table of Tables

Executive Summary

Project Goals and Objectives

3d printing has taken off as among both hobbyists and professionals as a way to quickly and easily create prototype or one-off parts. The most common form of 3d printing is Fused Deposition Modeling, or FDM, which extrudes heated plastic into the shape of a part. However, design of parts for this process is not well understood. There has been significant effort towards rules of thumb for creating designs that can be 3d printed, but little work that develops methods of stress analysis or mechanical design for the unique geometries that the process creates.

Therefore, the goal of this project was to create basic engineering tools for non-professional users. This will help close the technical gap in additive manufacturing, reduce waste, and create better trained users. This paper develops tools for effective analysis and testing of 3d printed beams and bridges. Experimental data are used to analyze and correct theoretical equations, ultimately producing models that can accurately describe these parts despite their anisotropy and geometry. A fixture for testing 3d printed truss bridges is constructed and tested in conjunction with another project, and is successfully used in an educational setting (Chamberlain & Meyers, 2016).

Summary of Beams

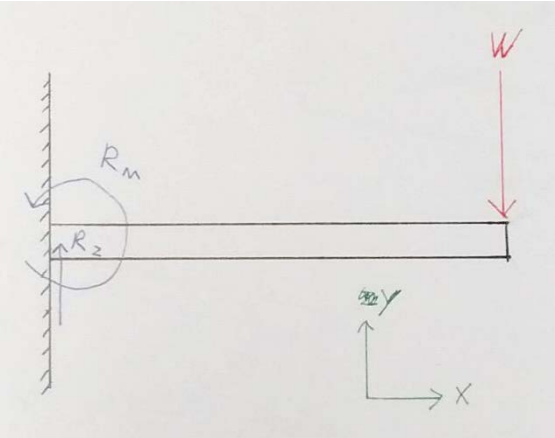

Figure 1: A simple beam in bending

Beams in bending are commonly taught in basic engineering courses. A straight beam is loaded perpendicular to its axis, causing bending (Norton, 2014). A simple sketch of a beam in bending is shown in Figure 1Figure 1: A simple beam in bending. Beam analysis is commonly taught in basic engineering courses, and can be used to model many simple situations. The equations for modeling these beams are well understood and accurate.

However, the assumptions that allow these equations to effectively model the beams do not apply to 3d printed parts, due to their anisotropy and infill. This project aimed to create a new model for calculating I_x, the area moment of inertia, which measures the strength of a cross section in bending. The model

developed is useful for both direct analysis, predicting the strength of a beam given a set of characteristics, and comparative analysis, measuring the change in strength of a beam as a characteristic is changed. There were three primary steps in this analysis.

1. **Create theoretical models of the beams.** Three models were created: a higher bound that modeled the beam as a solid bar, a lower bound that assumed a hollow shell, and an infill-based model that interpolated between the two.
2. **Break test specimens using an Instron to gather experimental data.** This data was compared to the theoretical models and used to compare their accuracy. A total of 36 specimens were tested, using four variables: part orientation, beam thickness and width, infill percentage, and number of shells.
3. **Adjust the theoretical models using the experimental data.** Both accurate and conservative estimates were made using the most successful model using linear scaling of the moment area of inertia.

Three theoretical models were developed.

- **Upper bound prediction:** $F_{max} = \frac{4I_x\sigma_b}{lh/2}, I_x = \frac{bh\text{^}3}{12}$. This equation assumes that the bar is completely solid, ignoring wall thickness and infill.
- **Lower bound prediction:** $F_{max} = \frac{4I_x\sigma_b}{lh/2}, I_x = \frac{bh^3}{12} - \frac{(b-2w_t)(h-2c_t)^3}{12}$. This equation assumes that the bar is a hollow shell, ignoring the infill.
- **Infill-based prediction:** $F_{max} = \frac{4I_x\sigma_b}{lh/2}, I_x = \frac{bh^3}{12} - (1 - \%I)\frac{(b-2w_t)(h-2c_t)^3}{12}$. This equation linearly interpolates between the high and low predictions based on the infill percentage.

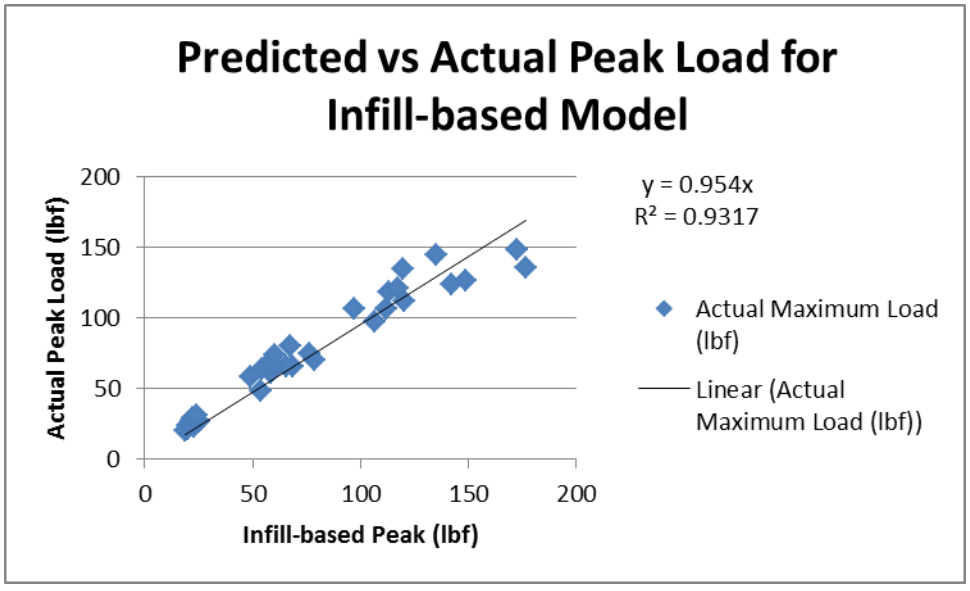

Figure 2: Predicted vs Actual Peak Load for Infill-based Model

Of the three models, it was found the proposed infill-based model was the most accurate, shown in Figure 2. The X axis shows the predicted peak load of the beam, while the Y axis shows the actual peak load. Linear adjustments to the model were made to provide both a more accurate fit, and to provide a

conservative estimate of part strength. The following equation for I_x is therefore proposed: $I_{x\,infill} = k\left(\frac{bh^3}{12} - (1 - \%I)\frac{(b-2w_t)(h-2c_t)^3}{12}\right)$, where $k = 1.05$ for the line of best fit and $k = 0.76$ for conservative analysis. This model is suitable for both direct and comparative analysis in most situations, though infill and outside part dimension comparative analysis generally over-estimates their effect on part strength. Further research should be done to better understand their relationship with strength.

Summary of Trusses

A system for effectively breaking 3d printed truss bridges was developed. This project experimentally determined the bridge dimensions to break cleanly and minimize printing time and material use, and designed a new load applicator for the testing device so it could effectively test the bridges.

There were four primary requirements for the new bridge testing device and format.

1. Make sure that the bridge format can be broken effectively on the device.
2. Create a bridge fixture that's compatible with the new device.
3. Figure out how we can create a new load applicator system that will apply point loads to two dimensional trusses.
4. Limit printing time and material use for the bridges.

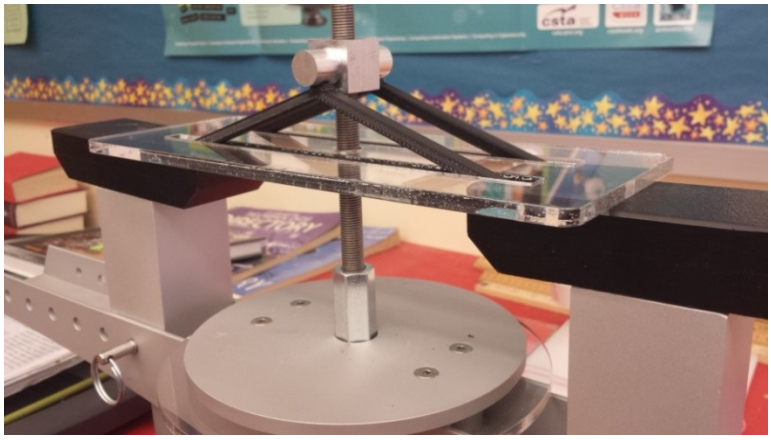

Figure 3: Bridge Testing Mechanism In Use

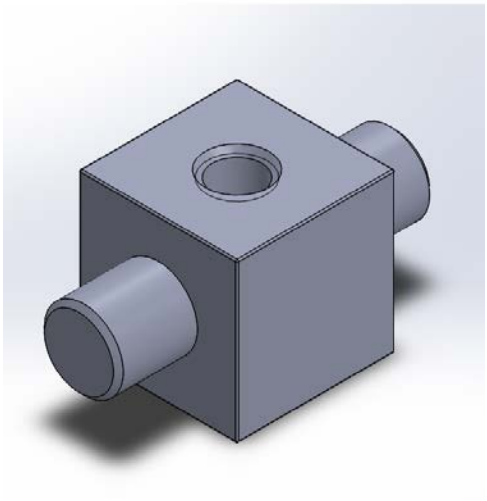

Figure 4: Testing Device for Truss Bridges

A new bridge testing mechanism was produced to help break 3d printed truss bridges, shown in Figure 3 and Figure 4. This model overcomes the limitations of the Pitsco Structures Testing Instrument that the high school had, allowing 2 dimensional trusses to be tested rather than the 3d popsicle stick bridges that it was originally built for. Bridges are placed on either side of the load applicator and compressed. A laser-cut acrylic plate helps align the bridges in place. However, it required two copies of the bridge to be printed for every test, which increased the printing time and material use.

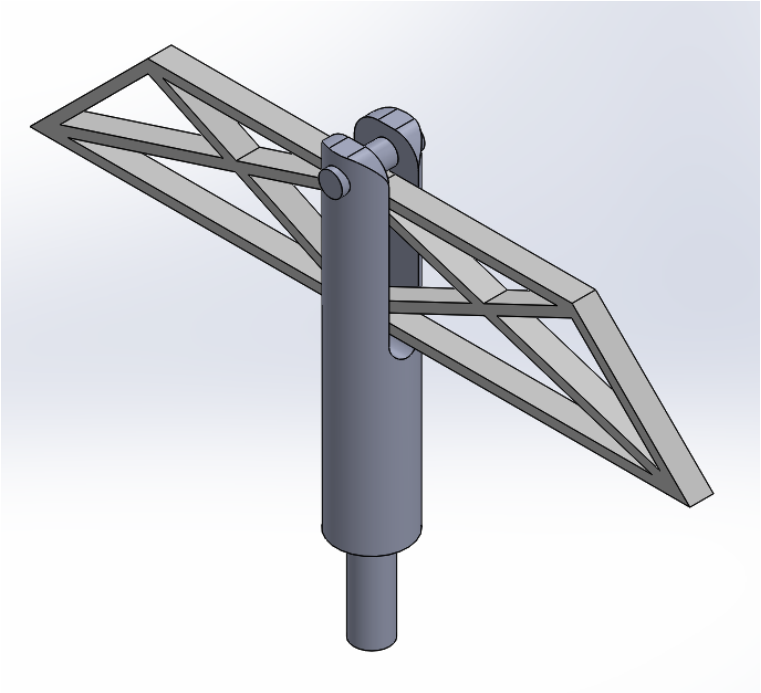

Figure 5: Proposed Truss Bridge Testing Device

To solve this, a new design was proposed, with a simple mockup shown in Figure 5. This design is more complicated to produce, but solves the printing time issue. A pin or shoulder bolt loads the bridge, which is inserted through a slot in the tester. The bottom portion is threaded, and attaches directly to the testing device.

Bridge dimensions were reached through iterative testing, finally settling on truss dimensions of 1.25” tall, 7” long, and 0.25” wide. Trusses had a width of 0.1875”. The model was printed lying flat to ensure optimum strength using a MakerBot Replicator 2x. Infill was set at 25%, but all other printing variables were left at MakerBot standard default settings, found in appendix 7.4 Full 3d Printing Parameters. These settings were found to produce good part strength that broke by snapping, and which had good stability under load. Thinner trusses tended to bend rather than snap or fall over under load, while thicker trusses were a waste of time and material.

1.0 Introduction

1.1 Objective

This paper develops tools for effective analysis and testing of 3d printed beams and bridges. Experimental data are used to analyze and correct theoretical equations, ultimately producing models that can accurately describe these parts despite their anisotropy and geometry. A fixture for testing 3d printed truss bridges is constructed and tested in conjunction with a concurrent project, and is successfully used in an educational setting (Chamberlain & Meyers, 2016).

1.2 Rationale

There are two main categories of additive manufacturing. First, there is the professional area using metal 3d printing like Selective Laser Sintering (SLS). This area employs very detailed engineering analysis, coupled with tools such as Computational Topography (CT), to create parts which are optimal for their function. Much of the work here has been in aerospace design, where the weight savings achievable through additive manufacturing are most important. The bar of entry is very high, since the machines and material are very expensive, and significant training is needed to create optimal designs.

On the other hand, there are plastic applications using Fused Deposition Modelling (FDM) machines, although technologies like stereolithography are also gaining prominence. The bar of entry for this is much lower, with many machines costing less than $1000. As a result, there's a significant hobbyist market. The design and analysis for these parts is generally more limited for several reasons.

1. The parts are generally not being used in critical applications, where optimizing and verifying the strength and weight of the part are crucial. As such, understanding the loads the part is experiencing, and how it will react to them is less important, and usually traded off for a shorter design cycle.
2. The nature of the process results in geometries which are very difficult to analyze, with anisotropic properties and complex infill support structures to reduce cost and speed manufacturing. These structures are inherently more difficult to analyze than bulk parts, even with advanced computational methods (which are themselves outside the reach of most hobbyist users.)
3. 3d printing has often been billed as a "rapid prototyping" process, due to the lack of setup costs and time. As a result, users often will just print a prototype design and test it to see if it works in lieu of applying engineering calculations. This form of "analysis by application" provides no other information besides a simple pass/fail binary, and can't be used to optimize part design. It also suffers from short tests, which don't take into account failure over time, and test loads which may not accurately resemble the problem (caused by the lack of problem analysis described in point 1.)
4. The hobbyist user base overall has little or no training in engineering principles, few available design resources, and no accessible training materials. Even if they wanted to do in-depth analysis, they don't have the tools available to do so. See 1.3 State of the Art for discussion of available training resources.

The end result of this is a process that isn't fully understood, producing parts which haven't been analyzed, for applications that aren't specified, operated by users who don't fully grasp any stage of the problem. The parts aren't optimized, wasting time and materials to manufacture. They are likely to fail due to the shortcomings of the "analysis by application" method. And, perhaps most critically, the users don't get the knowledge of engineering and manufacturing that they could from a detailed analysis. This is incredibly urgent right now, given the major lack of engineering and manufacturing employees across the United States.

However, these difficulties are not independent. The last point, the lack of engineering knowledge and resources, is the root cause for the other three. If the users had the knowledge and resources, they could effectively analyze their designs theoretically, rather than relying on trial and error design. While the anisotropy and infill are difficult to analyze compared to bulk solid parts, full analysis of the process could create effective design tools which would help to mitigate the problem. When all these points have been met, the designers will have a more complete understanding of their parts' performance, allowing them to be applied in increasingly critical positions. Furthermore, the lack of engineering expertise is self-reinforcing: because there aren’t tools to analyze the parts, and since it isn’t currently suitable for critical applications, FDM is less attractive as a manufacturing process, so engineers don’t use it.

Therefore, the goal of this project is to create basic engineering tools for non-professional users. This will help close the technical gap in additive manufacturing, reduce waste, and create better trained users.

1.3 State of the Art

1.3.1 Analysis of 3d printed parts

This section summarizes the research that has been done on analysis of 3d printed parts. Academic and non-academic research are investigated separately, due to the differing groups that have access to the information. This section provides a brief overview of the various research that was found and its general trends. A full list of the located research can be found in appendices 7.1 Full List of Academic Research and 7.2 Full List of Non-academic Research.

In summary, the hobbyist group especially has a significant amount of resources available for how to optimize geometry for the process of FDM. However, these resources don’t extend beyond rules of thumb for how to avoid the basic limitations of the process and optimize printability of the part. There are few resources on basic engineering principles in 3d printing, optimization of parts’ functionality, or performing detailed design analysis. Several software tools are available for basic analysis, but none of them are intended to optimize part design for given exterior loads.

Most existing academic research, for both traditional and additive manufacturing, is targeted towards either academic or professional groups. It is therefore inaccessible to 3d printing hobbyists, who lack the technical background and database access to make use of them. The research has so far focused primarily on quantifying the anisotropic material properties, rather than providing detailed design strategies. The work on design strategies has generally focused computerized tools rather than experimental equations.

Research Methods

Scholarly papers and other academic research were located using Google Scholar and the WPI Summon search engine. Publically available research was found with Google. When possible, the search was extended using the references and other links that the documents presented. Duplicate terms were used on each search engine for consistency. Following is a list of search terms:

- 3d printing design
- Additive manufacturing design
- FDM design
- Stress management in 3d printing
- Stress management in additive manufacturing
- 3d printing functional design
- 3d printing design for functionality

An industry magazine, Additive Manufacturing, focuses on 3d printing and is available for free online (Additive Manufacturing, 2016). However, while it does present case-studies from companies that perform AM, it doesn't discuss the engineering that they go through to develop their parts except in the most general sense. This isn't surprising as their development processes are proprietary. Additionally, as a magazine the information isn't formatted to provide a usable reference guide. Thus, though there is useful information for design and application of 3d printing, and it is publically available for free, the magazine was excluded from the State of the Art review after initial examination of the material.

Academic Research

There has been limited academic analysis of 3d printed parts. More research has been given to analyzing the material properties of the parts, especially their anisotropic properties. A good example is a senior research project from Rensselaer Polytechnic Institute. Robert Sayre III printed a large number of test samples with different printers and performed 3 point bending tests on them (Sayre, 2014). He then modeled the parts as anisotropic materials in Abaqus, a commercial Finite Element Analysis (FEA) package. By iterating the simulation with different anisotropic material parameters, he was able to come up with a close approximation of the material's properties.

This builds off a number of studies that analyze the anisotropic nature of 3d printed parts. One of the most significant was a 2002 paper, "Anisotropic material properties of fused deposition modeling ABS" (Ahn, Montero, Odell, Roundy, & Wright, 2002). The authors compared the effects of different process variables on the strength of 3d printed parts under simple tension and compression loaded, and came up with six rules for optimizing the print orientation of parts. These are listed below:

1. Build parts such that tensile loads will be carried axially along the fibers
2. Be aware that stress concentrations occur at radiused corners. This is because the FDM roads exhibit discontinuities at such transitions
3. Use a negative air gap to increase both strength and stiffness
4. Consider the following issues on bead width
    a. Small bead width increases build time
    b. Small bead width improves surface quality

    c. Wall thickness of the part should be an integer multiple of the bead width to avoid gaps
5. Consider the effect of build orientation on part accuracy
    a. Two-dimension slices closely reproduce geometry
    b. Three-dimension layer stacking creates linear approximations
6. Be aware that tensile loaded area tends to fail easier than compression loaded areas

Most of the work focusing on design principles has looked at very high-level principles and assemblies. In a 2014 paper, Christoph Klahn, Bastian Leutenecker, and Mirko Meboldt discuss how 3d printing could allow increased design freedom and improved part design (Klahn, Leutenecker, & Meboldt, 2014). One paper proposes design principles for rapid prototyping force sensors (Kesner & Howe, 2011). The scope of this work is very limited, and it doesn't move beyond very simple rules of thumb for the designs.

Other work has focused on optimizing printing strategies. A 2014 talk at SIGGRAPH proposes new strategies for support structures (Dumas, Hergel, & Lefebvre, 2014). There is some work on design for external loads, but it uniformly focuses on computerized models that are inaccessible for non-professional users, and only discusses changing print strategy, rather than adapting part shape to the loads. One 2015 paper discusses optimizing internal support structures for external loads (Zhang, et al., 2015).

Non-academic Resources

The most in-depth non-academic resource specifically for 3d printing is a self-published book by Clifford Smythe, entitled "Functional Design for 3D Printing 2nd edition: Designing 3D printed things for everyday use" (Smythe, 2015). The document discusses how the 3d printing process affects parts, and some of the ways to design around the process's limitations. Its main subjects are:

- The 3d printing process and variables
- Limitations and printability factors
- Design strategies and structures
- Aligning and fastening assemblies
- Common design features and more advanced strategies
- Rules of thumb for part fit
- Slicer manipulation
- Printer calibration
- Experiments with strength: anisotropic strength between layers, and infill

However, while the book provides a good basic introduction to 3d printing, and proposes many interesting strategies, it provides little information on how to actually analyze or implement them. For example, Smythe describes a method of strengthening parts by putting microholes through critical areas, essentially forcing increased infill, but there is no description of how to determine what areas need said holes, or how the optimal pattern and size can be determined. Similarly, his discussion of engineering features describes the various features, but gives no actual tools for designing them. The book is thus more useful for an experienced user looking for design ideas than as a design reference. Furthermore, most of the book is about design for printability or how to tweak existing designs rather than the design process as a whole.

His experimental data, presented in an appendix, are useful to demonstrate concepts, but functionally useless for design purposes. The anisotropic experiment shows two different designs for the same part, one single piece and the other made of two pieces to take advantage of the anisotropy, and compares their failure strength. While the results conclusively demonstrate Smythe's point that using parts in their strongest orientation is a good idea, it provides no quantifiable data that can be used for further design.

Other than this book, there are several other resources available over the internet. Most of the commercial 3d printing services, such as Shapeways, have design guides that describe the different features they can produce, manufacturing tolerances for different materials, ways to improve printability, and common model problems in the STL part files (Shapeways, 2015). However, they don't extend this to discuss functional design for the parts.

There has also been significant work put into automated tools for assisting 3d printing design, largely from companies in the 3d printing market. A paper from Adobe Systems Incorporated and Purdue University describe new computational tools for computing weak points in 3d printed models and automatically strengthening them (Stava, Vanek, Benes, Carr, & Mvech, 2012). The tool identifies weak points the model using cross-sectional areas, calculates the most vulnerable based on the weight of the model or applied outside load, and automatically thickens the weak areas, adds struts, or hollows out the model in order to reduce stress in the weak areas. A similar tool, developed by members of Autodesk Research, identifies the thinnest areas of the model and lets users interactively strengthen those sections, then calculates the optimal printing orientation for strength in the weak areas (Umetani & Schmidt, 2013).

While these tools have promise in the future, they're currently not as useful for engineering purposes. First, the methods that they use to calculate stress aren't exact. Rather than accurately modelling the part with its infill structure, they instead just use cross-sectional areas. As such, it's not an accurate model of the part usable design verification in critical applications. The target application is mostly to improve printability of fragile models. Second, the algorithms aren't optimal for handling outside forces, since they're mostly intended to make sure that the part is printable and can stand up under its own weight. Third, it doesn't provide the user with the tools to understand the forces being applied. If the situation that's modeled doesn't reflect reality, then the optimized results aren't going to work properly. Lastly, these solutions do nothing to educate the designer about how they can improve their design or better understand how the model interacts with the applied forces.

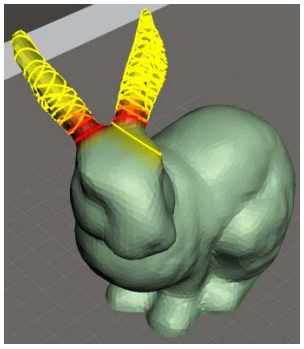

Figure 6: Weak sections identified by Autodesk MeshMixer

Similar tools are already in some software, such as the free Autodesk MeshMixer. Shown in Figure 6, it uses the same cross-sectional area identification to find vulnerable parts of the design. Other tools identify optimum printing angle and potential overhang issues and generate support structures. While these tools are useful for improving the printability of parts, they still provide little assistance for functional design in response to outside stresses.

1.3.2 Beams in Bending

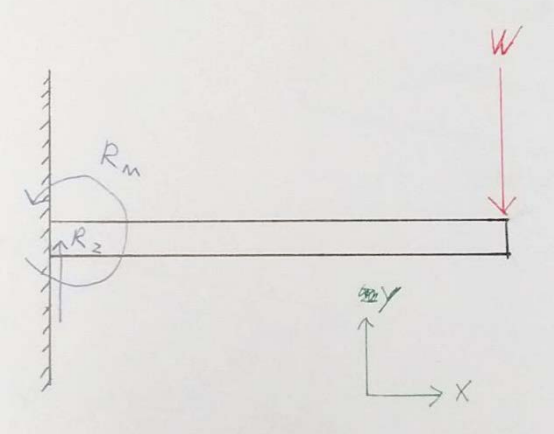

Figure 7: A simple beam in bending

The simple model of a beam in bending assumes pure bending loads with no tensile forces (Norton, 2014). A simple sketch of a beam in bending is shown in Figure 7. Beam analysis is commonly taught in basic engineering courses, and can be used to model many simple situations.

The standard equation for modelling the breaking strength of a rectangular beam in 3-point bending is $F_{max} = \frac{4I_x\sigma_b}{lh/2}$, where $I_x = \frac{bh^3}{12}$ is the moment area of inertia, σ_b is the tensile failure stress of the material, l is the supported span of the beam, and b, h are the width and height of the beam respectively.

However, this equation assumes a constant value for I_x. In a 3d printed beam, this is not the case, because it varies with the infill throughout the length. This makes it much more difficult to analyze, since every point in the beam must be analyzed for failure rather than simply the point of highest stress as the previous theoretical equation does.

1.3.3 Truss Bridges

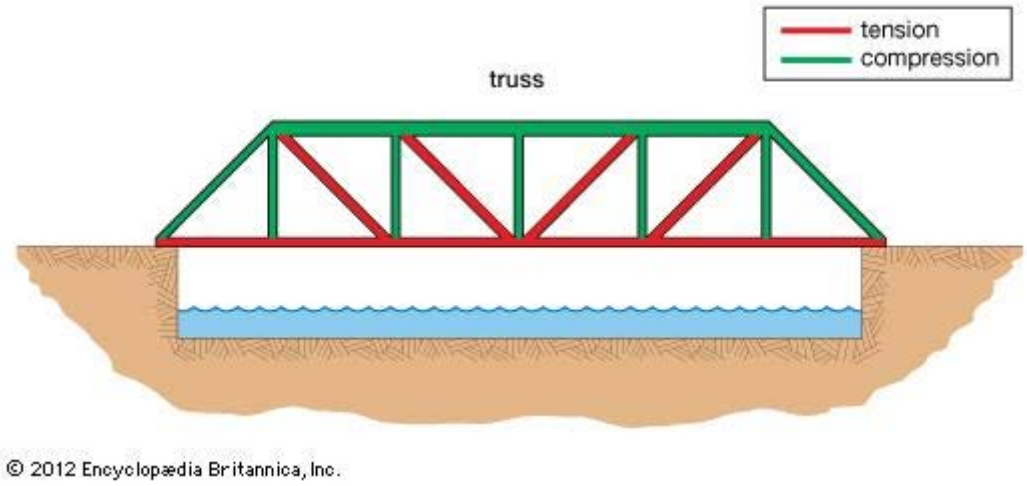

Figure 8: Truss bridge showing loading of members (Encyclopaedia Britannica, 2016)

The truss is a standard introductory model that is commonly used to simulate bridges (Norton, 2014). They make the assumption that the members are held together with pin joints, which makes it so they are subjected only to tensile or compressive loads. This makes them simple to analyze: sum the forces at every joint, and solve the resulting set of equations for the internal forces in every member. This simplicity makes them useful as a first introduction to engineering design and analysis. The model is fast and easy for students to analyze, helping to grasp initial concepts before moving on to more complicated problems.

However, the assumption about pin joints is inaccurate for 3d printed parts. Pin joints are made of multiple pieces that are able to freely rotate and experience no moments or bending. In contrast, 3d printed trusses have rigid blocks that apply loads practically only through bending and moments at the base of each beam. As a result, the pin joint model doesn't accurately describe 3d printed parts.

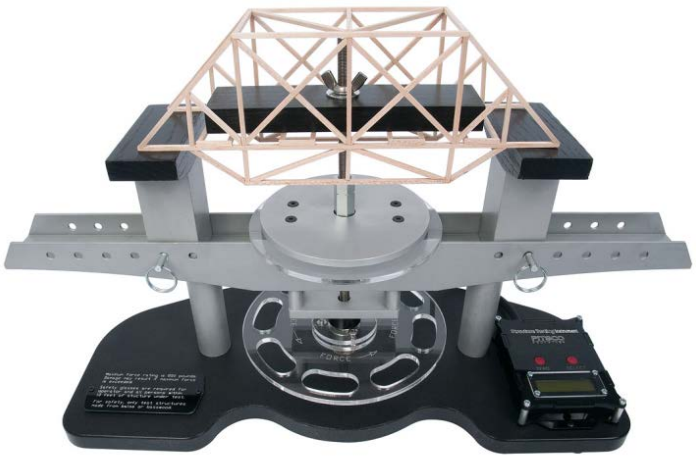

Figure 9: Pitsco Structure Testing Instrument (Pitsco Education, 2016)

There are also issues encountered with the devices used to test the trusses. This project collaborated with an IQP working to integrate 3d printing into high-school curricula (Chamberlain & Meyers, 2016). The setup was determined by the school that the IQP was working with, which had a Pitsco Structures Testing Instrument, shown in Figure 9 (Pitsco Education, 2016). This device was specifically designed for testing structures and bridges in an educational setting. Load is applied by turning the wheel at the bottom, which pulls a 3/8”-24 threaded rod down, compressing the part via a load applicator attached at the top (a rectangular bar for distributed loads in the above image.)

However, there are a few issues that make it not ideal for 3d printed parts.

- It’s designed for use with three dimensional trusses. The students had only been working with 2d cross-sections, since those are easier to design and print. Full 3d trusses would be much weaker, more time-intensive to design and analyze, and require much longer to print and assemble.
- It’s designed to apply distributed loads using a load block like shown. However, point loads are another one of the major assumptions that the truss model makes. Even if the truss model is inaccurate, conditions should be kept as close to it as possible so it provides the best approximation possible. Point loading also lets us give the students more design freedom, because we only need to require a single point that load can be applied on, rather than a whole area.
- Third, the load applicator threading onto the rod is inconvenient as designed, since it must be backed all the way off and on to load a new part.
- It has no way of capturing deflection information. While this is not a critical failure, it would be useful data to capture.

1.4 Approach

Two main areas are targeted in this project: truss bridges and beams in bending. The two sections of the project were largely separate, and used different strategies to pursue their goal.

The main focus for the truss section was on creating a working system for breaking 3d printed truss bridges in an educational setting. The first component of this was the guidelines for the bridge design to ensure that they could be effectively broken. This was reached iteratively, experimenting with bridge dimensions and part settings until a satisfactory set of guidelines was reached. The second component was the test fixture. Modifications were made to the existing testing device to ensure that it could effectively break the bridges, since they differed in notable ways from the structures the device was intended for.

This project sought to create a simple equation to accurately model the breaking strength of 3d printed beams. The analysis here focuses on geometry-based variables rather than other printing characteristics so as to provide the most general possible solution. This contrasts with most previous research which has primarily examined the anisotropy and printing variables.

There were three main steps in this analysis. First, a theoretical analysis of the beams was used to identify key geometry variables. These variables were then experimentally tested to determine their effect on part breaking strength. Lastly, the experimental test results were analyzed and used to modify the theoretical equation to provide a more accurate fit.

Equations were tested with two main criteria: first, they must be able to directly predict the strength of a beam of some design, referred to as direct analysis. Second, they must be able to predict how beam strength will change as design variables are altered, referred to as comparative analysis.

2.0 Methods

In this section, the specific methods used for the research will be discussed. The goal of this project was to develop tools for design and analysis of 3d printed parts. Specific areas and tools that should be focused on were identified with three main criteria.

1. What tools and models are most commonly used and provide the greatest utility? Primary focus must be given to the tools that are most generally useful.
2. What tools and models are most basic and fundamental? Since the aim of this project is to develop tools for people without engineering backgrounds, it is important to focus on areas that both do not require a great deal of technical understanding to grasp and which provide a good starting point for future work.
3. What tools and models do not accurately describe additively manufactured parts? This identifies the tools that need to be adapted to FDM parts.

Two areas were selected for analysis based on these criteria. First, truss analysis was chosen, due to its importance to the related IQP project and because it serves as a good introduction to engineering design. Second, beam bending was chosen as a fundamental engineering model that's commonly presented shortly after trusses, and which is of great use in designing parts.

2.1 Beam testing and analysis

There were three main sections involved in the analysis of beams. First, theoretical models were developed, allowing them to be compared to traditional equations, and identifying useful variables. Second, sample beams were printed and tested to gather empirical data on their breaking points. Lastly, these data were analyzed and used to adjust the theoretical models to better provide accurate predictions.

2.1.1 Theoretical Modelling

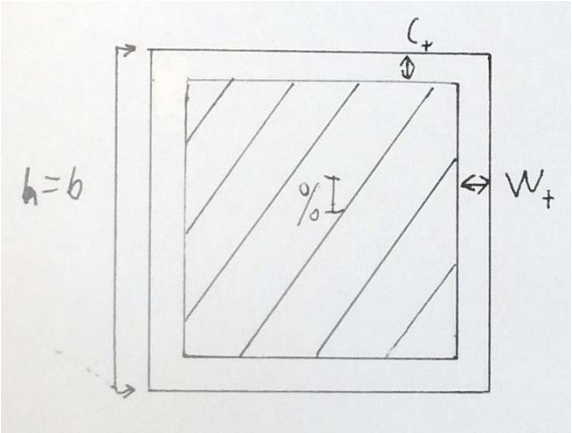

Figure 10: Cross-section of 3d printed beam

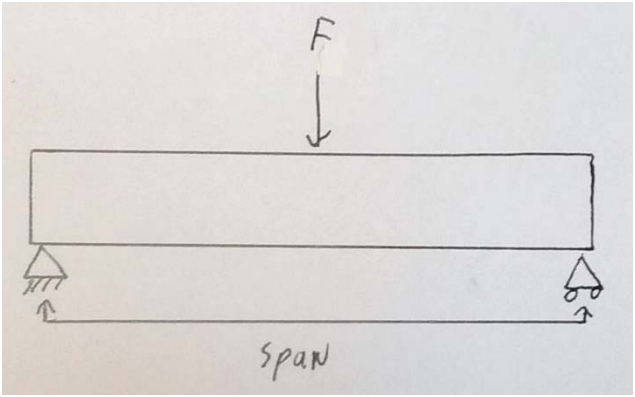

Figure 11: Setup for 3-point bending tests

Theoretical analysis on the beams was undertaken to develop an initial model and identify variables for experimentation. Figure 10 shows the cross sectional drawing used, and Figure 11 shows the 3-point bending setup. This analysis used traditional beam equations to develop high, low, and intermediate predictions for failure strength in 3-point bending based on differing moment areas of inertia, shown below. The high projection assumed a solid beam, the low projection assumed a completely hollow beam, and the infill-based projection interpolated linearly between the high and low projections based on the infill percentage. Traditional beam equations were used to model the breaking strength given these assumptions (Norton, 2014). Full derivation of these equations can be found in appendix 7.5 Detailed Derivation of Beam Strength Predictions.

- High prediction: $F_{max} = \frac{8I_x\sigma_b}{lh}, I_x = \frac{bh^3}{12}$
- Low prediction: $F_{max} = \frac{8I_x\sigma_b}{lh}, I_x = \frac{bh^3}{12} - \frac{(b-2w_t)(h-2c_t)^3}{12}$
- Infill-based prediction: $F_{max} = \frac{8I_x\sigma_b}{lh}, I_x = \frac{bh^3}{12} - (1-\%I)\frac{(b-2w_t)(h-2c_t)^3}{12}$

The equations break the problem up into two main parts. First, there is the moment area of inertia I_x. The calculations for this depend on the cross sectional geometry of the beam, which is usually what the

designer needs to optimize. This is dependent on the outside dimensions of the beam (b, h), infill ($\%I$), ceiling thickness (c_t), and wall thickness (w_t).

Second, the calculated I_x value is used to calculate the breaking strength, deflection, and any other information required. In addition to the moment area of inertia, these calculations require information on the constraints placed on the beam: the span of the beam (l), what forces it is placed under (F), and the tensile failure strength of the part (σ_b). The designer usually has little control over these constraints, since they are specified by the required application.

Since these two sections of the calculations are discrete, it is easier to separate the behavior of the 3d printed beam from the specific design constraints, allowing the equations to be more generalizable. As a result, the theoretical model and the experimental modifications are all focused solely on the calculation of the moment area of inertia. This can then be used in any standard beam bending formula that may be necessary.

2.1.2 Empirical Testing

Based on the theoretical analysis, three geometry variables were identified for testing 3d printed beams to develop an empirical model for beam analysis and displacement: the outside part dimensions, infill percentage, and wall shell thickness. One additional variable was included to more effectively analyze the anisotropy, the part orientation.

One geometry variable was rejected, the floor/ceiling thickness, because its effects are relatively simple to predict, and because its behavior is largely captured by the wall thickness when the part is oriented with the walls on top and bottom.

Following is descriptions of the variables analyzed and how testing values were selected.

Outside part dimensions: all samples had square cross sections, chosen because most beams in actual applications are, if not square, fairly close to it. Outside dimensions of 0.25”, 0.375”, and 0.5” were analyzed. Beam thickness was kept low to fit within the maximum load of the testing machine.

Infill percentage: Four separate infill percentages were used, with values of 10%, 20%, 40%, and 60%. These cover the general range of use that doesn’t get time- and cost-prohibitive to use.

Wall shell thickness: Three shell thicknesses were used, with thicknesses of two, three, and four shells. Increasing shells above this point would have essentially made the smallest test samples solid bars, which is not a case that was considered in this study.

Printing orientation: Two separate printing orientations were tested, one with the printing axis oriented along the axis of bending, and the other with it oriented perpendicular to the axis of bending and the axis of the beam. The third potential orientation, with the printing axis along the beam axis, was rejected because of the large effects that anisotropy would have on its strength, making it less useful.

The parts were printed without rafts to reduce printing time. Other than the rafts and testing variables, all printing variables were left at the default MakerBot settings for the MakerBot Replicator 2x used. A full list of these settings can be found in appendix 7.4 Full 3d Printing Parameters. All samples were printed from red MakerBot ABS filament.

Infill percentage and wall shell thickness were judged to be independent and were not tested together. Full factorial analysis was performed other than this constraint (Barrentine, 2014). There were 42 theoretical samples. Six samples were redundant between the shell thickness and infill tests, and were eliminated. This resulted in 36 final testing samples.

Figure 12: Instron 5544 used for testing

Beams were tested in 3-point bending on an Instron 5544 with a 3-point flexure fixture, shown in Figure 12. The machine's load cell has a maximum load capacity of 450lbf. Span was kept constant for all parts at 2.514 inches. Load was applied with constant extension rate of 0.5 inches/minute. A slight preload of 1lbf was applied before starting the test to keep the part firmly in place, and the extension was zeroed at this point. The load cell was balanced before every test with the subject on the fixture, but before the preload had been applied. Data collection was continued until the load had decreased 40% from its peak value. Breaking strength was read from this peak value.

ASTM standards per D790-15 were intentionally not followed for several reasons (ASTM International, 2016).

1. The standard is only for solid specimens, which means that the stress analysis methods specified do not produce accurate results.
2. The suggested support span-to-depth of 16:1 for thermoplastics would produce very high bending in these beams, making it difficult to analyze the breaking point.
3. The outside dimensions proposed are 0.5" wide by 0.125" thick, which is not suitable for analyzing the effects of infill, and does not closely match the shape of most beams in practice.
4. They recommend a minimum of 5 specimens of each size. While this would be ideal, the number of different specimens and conditions made this prohibitive, while simultaneously providing much of the redundancy that multiple specimens would provide.

5. They specify a maximum of 0.10 inch/inch-minute crosshead feed rate for the test. This is useful when the purpose of the experiment is to determine material characteristics as accurately as possible. However, the intent of this project is to provide equations for beams under normal circumstances, which does not include slowly-applied loads.

2.1.3 Data Analysis

Data were analyzed with modified versions of standard testing techniques. These methods were chosen over standard effect analysis due to the anticipated non-linearity of data (Barrentine, 2014).

To analyze the models' suitability for direct analysis, predicted and actual load values were compared, rather than undergoing factor analysis. The linear slope of the line of best fit was applied as a linear correction factor, and this corrected model was used for calculating the error of the model.

To predict the usefulness of models for comparative analysis, individual variables were analyzed by normalizing predicted and actual load values to base data points. This analyzed the ratio of part strength provided by changes in variables. Error was calculated between these predicted and actual ratios. For all comparative analyses, base samples were not used to calculate the error, since they always have an error of 0.

By directly comparing the predictions to actual data, the ideal model is always a linear fit with a slope of 1 and a Y intercept of 0, and deviations away from this can be easily analyzed. This was aided by forcing all linear fits to go through the origin. Linear scalar factors were thus the only compensation that must be considered, making analysis and comparison easy. It also has the advantage of being unit-independent. While load values and dimensions are presented in Imperial units, all equations and correction factors proposed function regardless of units.

2.2 Truss design and modeling

Two major influences drove the selection of trusses as one of the models for analysis. First, they are useful as a first introduction to engineering design and analysis. The simplicity of the model makes them fast and easy for students to analyze, helping to grasp initial concepts before moving on to more complicated problems.

Second, one of the major sections that the IQP focused on was on truss bridge analysis, with students designing and building their own truss bridges, and then breaking them to test the strength (Chamberlain & Meyers, 2016). This was intended to create greater interactivity for the students.

The goal of this section of the project is to facilitate the high school's experiments. A testing setup was designed to effectively test the truss bridges. This testing setup was used to break example bridges and bridges of students' design. See the IQP report for more information on this project.

There were four main objectives for the new setup.

1. Make sure that the bridge format can be broken effectively on the device.
2. Create a bridge fixture that's compatible with the new device.

3. Figure out how we can create a new load applicator system that will apply point loads to two dimensional trusses.
4. Limit printing time and material use for the bridges.

Three designs were proposed and examined for use.

1. Have a cantilevered load applicator that applied load to a bridge on one side of the threaded rod. This was rejected for stability purposes, since the bridges should be as thin as possible to reduce material use and they could fall over, ruining the test. The cantilever loads could also cause damage to the machine.
2. Print wide bridges with holes through the center for the rod. This would take a massive amount of material to print each bridge, and would create stress concentrations at the center of the bridge that would invalidate the results.
3. Have structures on both sides with some sort of bridging material that would distribute the load. This requires that bridges be printed for both sides of the device, doubling material use and printing time.

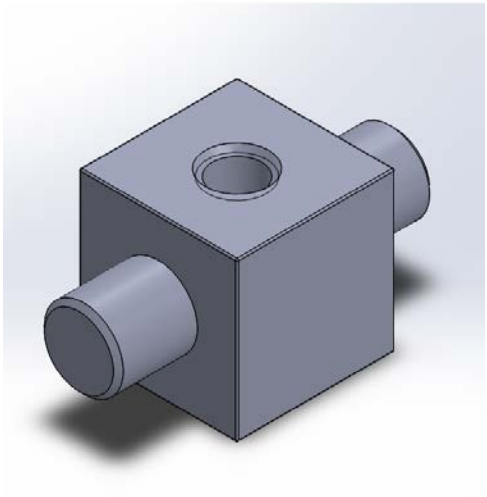

Figure 13: Testing device for truss bridges

While non-optimal, design three was chosen due to its simplicity and reliability. A model of the load applicator can be seen in Figure 13. The block was machined out of aluminum to ensure that it is significantly stiffer and stronger than the ABS bridges, and threads directly onto the threaded rod. Bridges sit under each cylindrical boss, which apply the load.

Bridge dimensions were reached through iterative testing, finally settling on truss dimensions of 1.25” tall, 7” long, and 0.25” wide. Trusses had a width of 0.1875”. The model was printed lying flat to ensure optimum strength using a MakerBot Replicator 2x. Infill was set at 25%, but all other printing variables were left at MakerBot standard default settings, found in appendix 7.4 Full 3d Printing Parameters. These settings were found to produce good part strength that broke by snapping, and which had good stability under load. Thinner trusses tended to bend rather than snap or fall over under load, while thicker trusses were a waste of time and material.

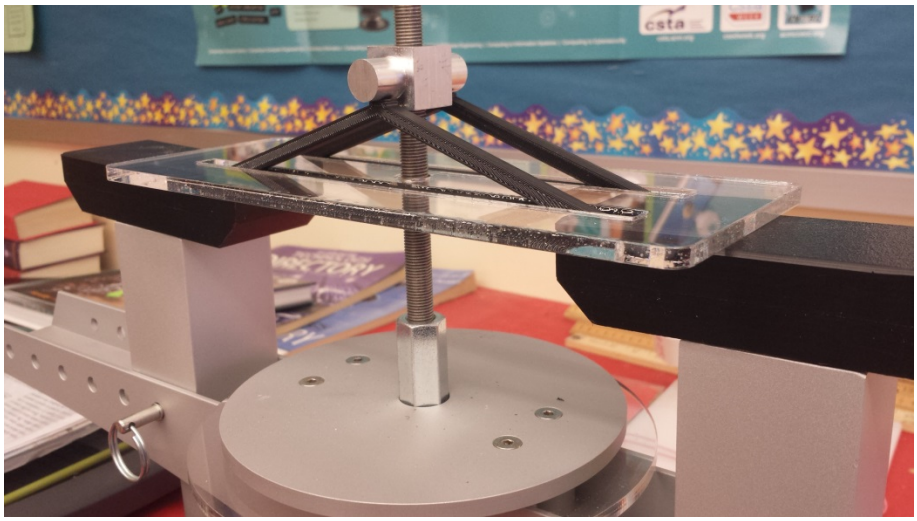

Figure 14: Bridge tester in use

Figure 14 shows the bridge tester in use, with two example trusses loaded under the load applicator. A laser cut acrylic plate was used to help align the bridges, and did not support the bridges in use.

3.0 Results

This section presents the data and analysis from this project, and discusses the issues encountered.

3.1 Beam Analysis

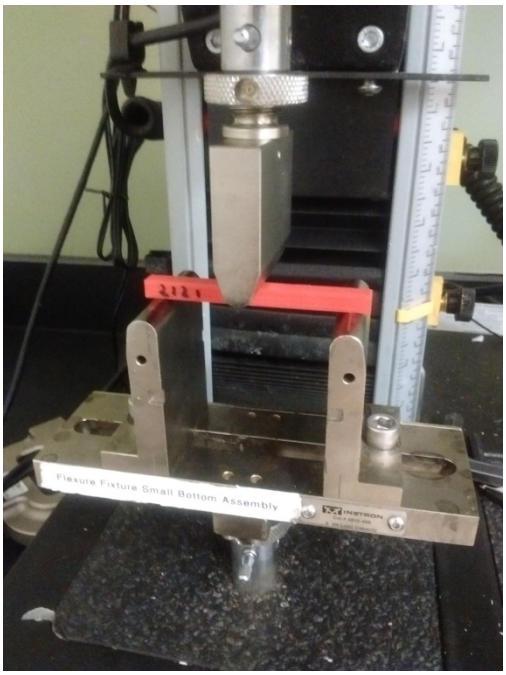

Figure 15: Beam Testing Apparatus in Use

Beam testing was completed without issue. No samples were excluded from the final analysis. A picture of the testing apparatus in use is shown in Figure 15. The theoretical predictions can be found in appendix 7.7 Predicted Beam Data, and the full data from empirical tests can be found in 7.8 Raw Data from Beam Testing.

3.1.1 Upper Bound Analysis

The upper bound model for calculating I_x universally overestimated the strength of the beams. This model assumes that the bar is a solid piece of ABS, ignoring the hollow inside entirely.

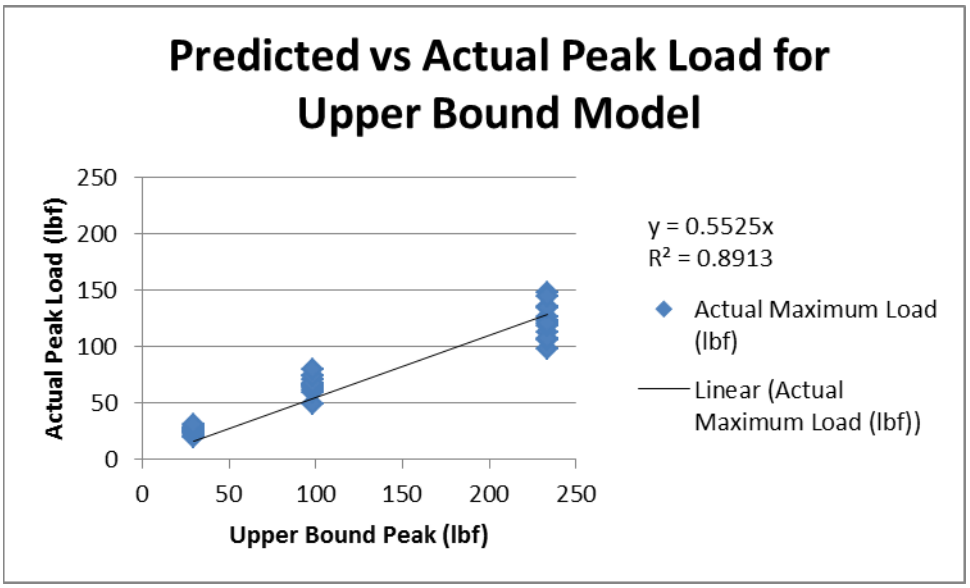

Figure 16: Predicted vs Actual Peak Load for Upper Bound Model

Figure 16 shows the predicted versus actual breaking strength for upper bound breaking strength model. The small red dots show the predicted load, while the large blue dots show the actual breaking load. Both are graphed relative to the predicted maximum load: thus, a slope of 1 indicates that the results align perfectly. The upper bound analysis consistently overestimated part strength by nearly two times.

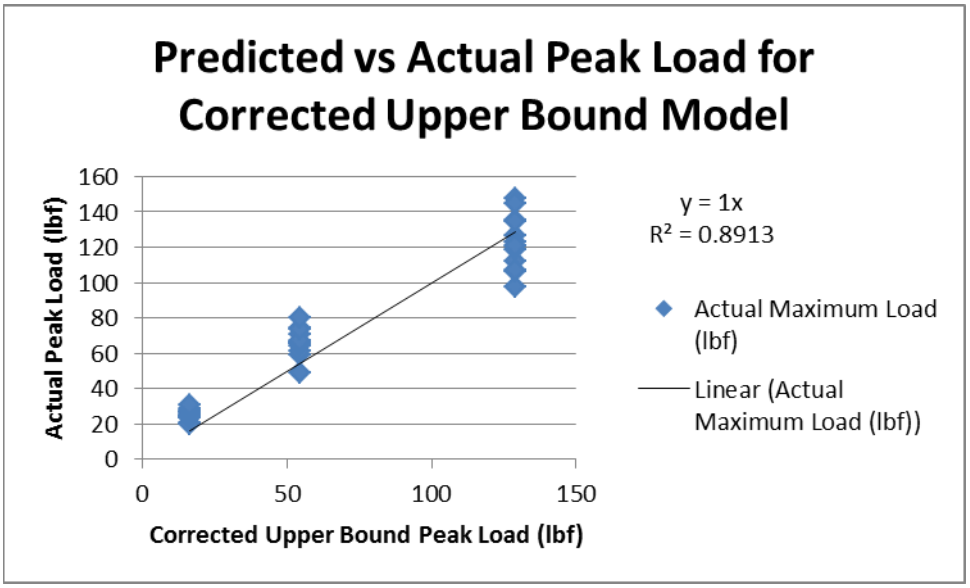

Figure 17: Predicted vs Actual Peak Load for Upper Bound Model

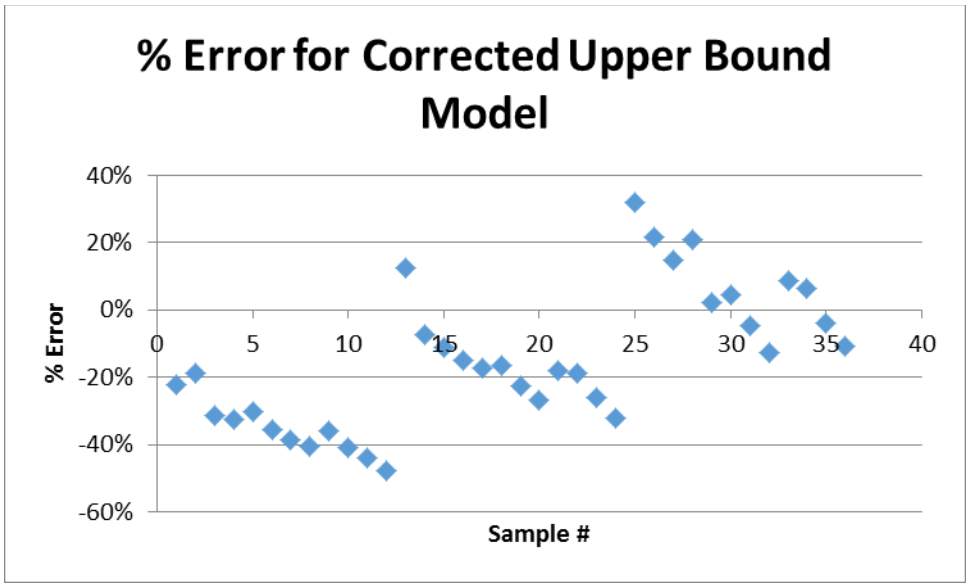

Figure 18: % Error for Corrected Upper Bound Model

Even corrected for this linear error, the model still isn't accurate, as shown in Figure 17 and Figure 18. The peak error is -48%, with an average error of -15%, and an average absolute error of 22%. This is far too high to be useful for direct calculation of part strength, outside of simple order of magnitude calculation.

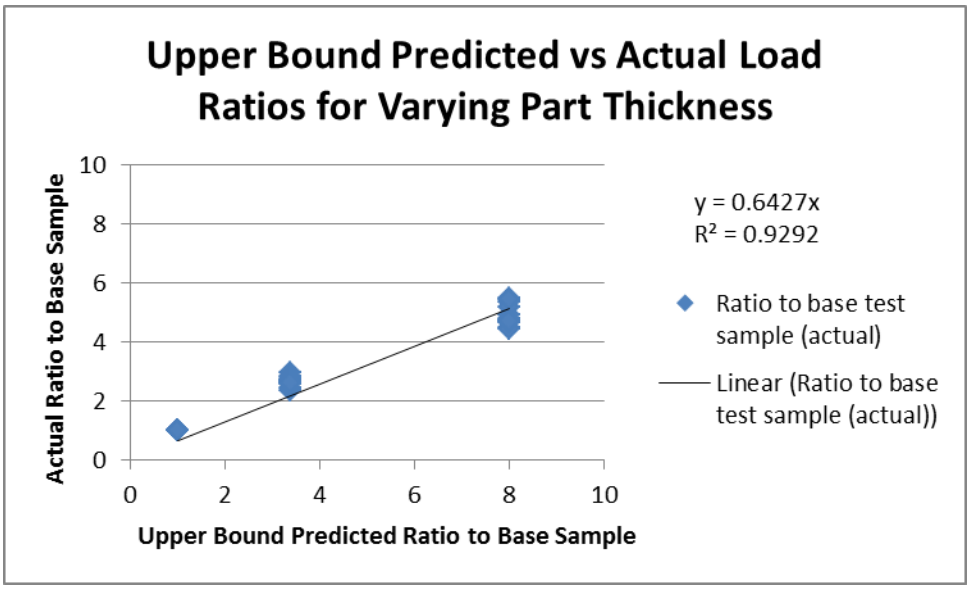

Figure 19: Upper Bound Predicted vs Actual Load Ratios for Varying Part Thickness

The model consistently overestimates the impact of changes in part size, as shown in Figure 19. This graph compares the predicted increase in strength over smaller samples with the actual increase. Again, a one-to-one slope would represent a perfect match. The upper bound model overestimates the change by roughly 50% over actual values. Average and average absolute errors were both 46%, and peak error was 80%. For all comparative analyses, base samples were not used to calculate the error, since they always have an error of 0.

Because the upper bound model does not use the infill percentage, orientation or wall thickness as variables, its usefulness for comparative analysis for those variables was not analyzed.

3.1.2 Lower Bound Analysis

The lower bound analysis consistently under-predicted part strength. This model assumes that the part is a hollow shell, ignoring infill.

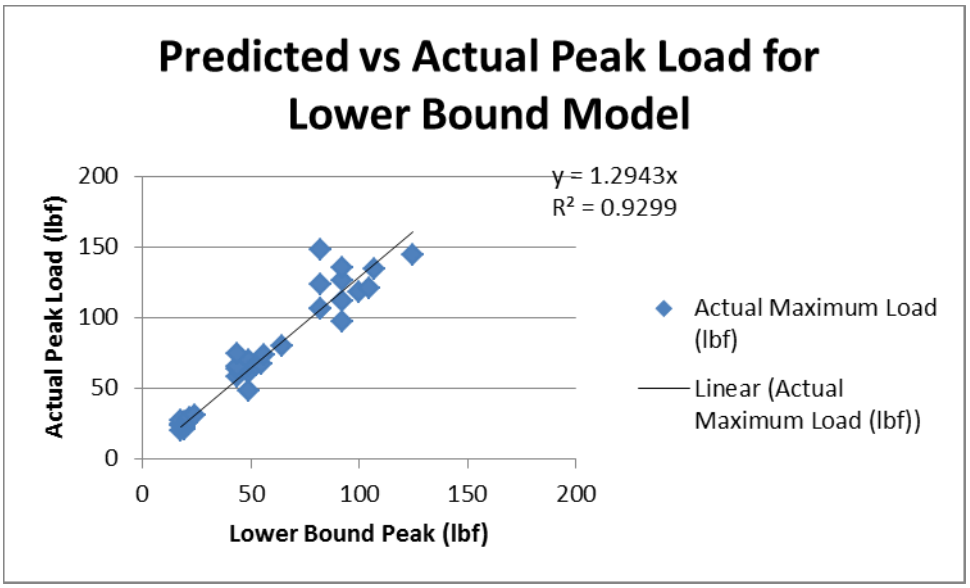

Figure 20: Predicted vs Actual Peak Load for Lower Bound Model

As shown in Figure 20, predictions from the lower bound model aren't close to actual results. They tend to under-predict results by about 24%, and there are some significant outliers caused by infill that it can't predict. However, the R^2 value is good at 0.9299, which shows that the data are fairly linear and can be corrected to improve the accuracy.

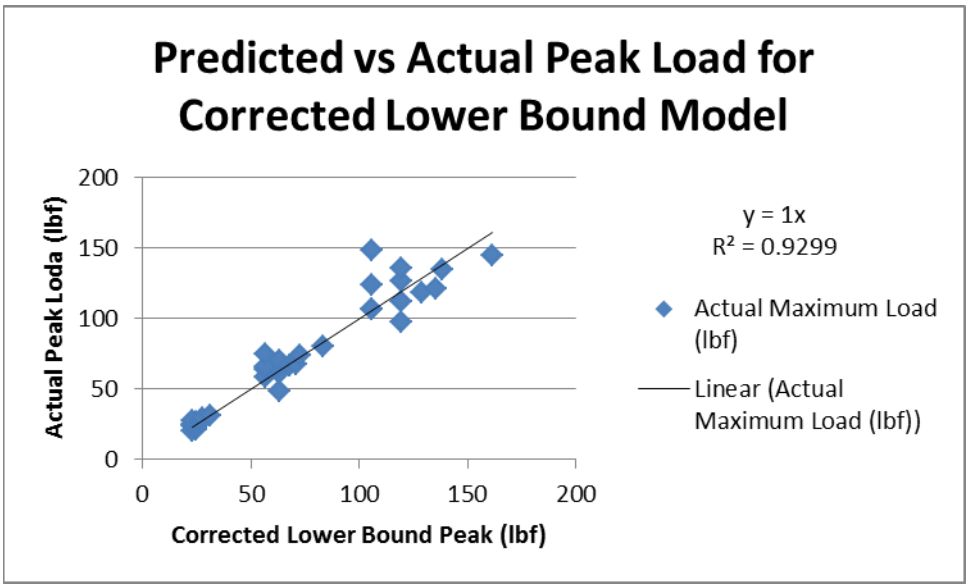

Figure 21: Predicted vs Actual Peak Load for Corrected Lower Bound Model

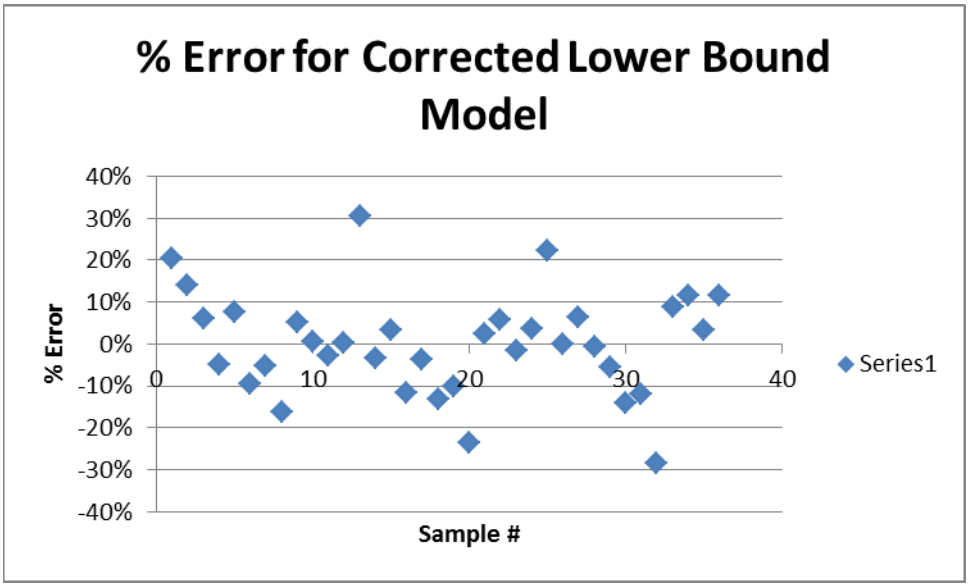

Figure 22: % Error for Corrected Lower Bound Model

When corrected, the model is on average fairly accurate, but has large peaks that make it undependable. The peak error is 31%, with an average absolute error of 9%. However, the average error was 0%, which shows that the error is symmetric.

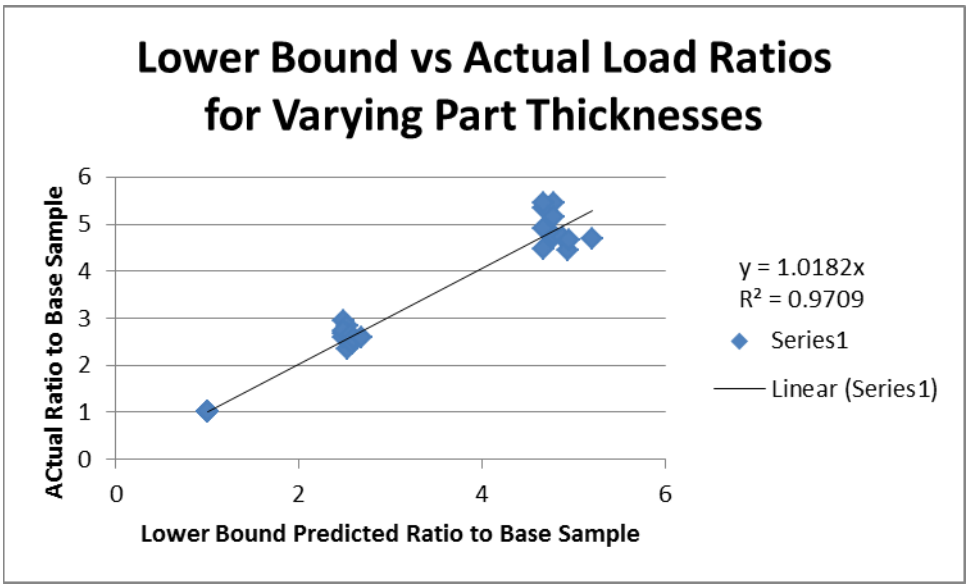

Figure 23: Lower Bound Predicted vs Actual Load Ratios for Varying Part Thicknesses

This model accurately predicts changes in part strength as part thickness changes, as shown in Figure 23, within 3% and R^2=0.9671. This makes the model very suitable for comparative analysis of strength when the size of the beam is being changed. There was a peak error of 14%, with an average error of 2% and an average absolute error of 8%.

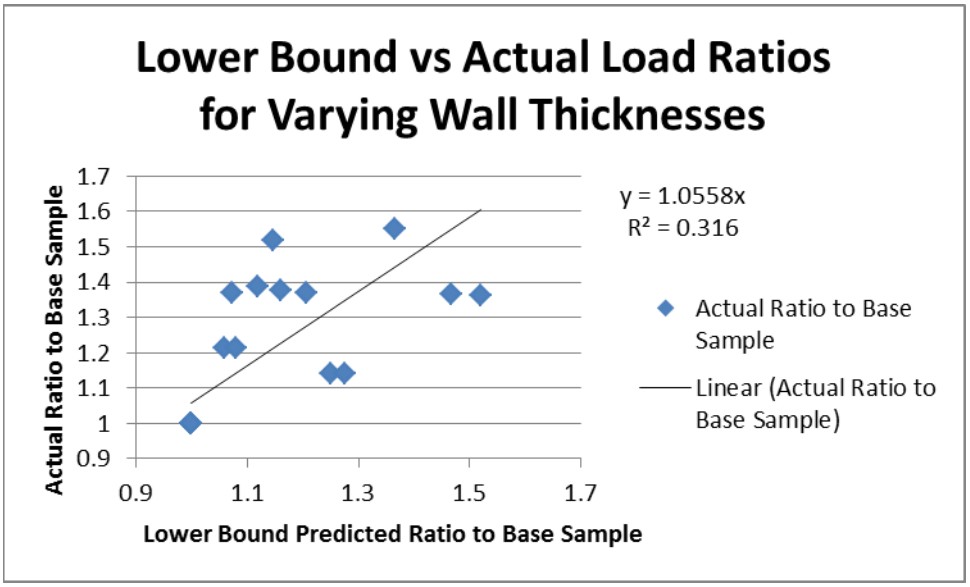

Figure 24: Lower Bound vs Actual Load Ratios for Varying Wall Thicknesses

However, it was less successful at predicting part strength as a function of wall thickness. While the trend matched closely, within 10%, the data were much noisier with an R^2 value of 0.316. The peak error was -25%, with average error of -7% and average absolute error of 14%. However, it is worth noting that the error trends negative, and all of the significant errors were negative. The highest positive error was only 10%. This shows that the model is generally conservative, which can be valuable.

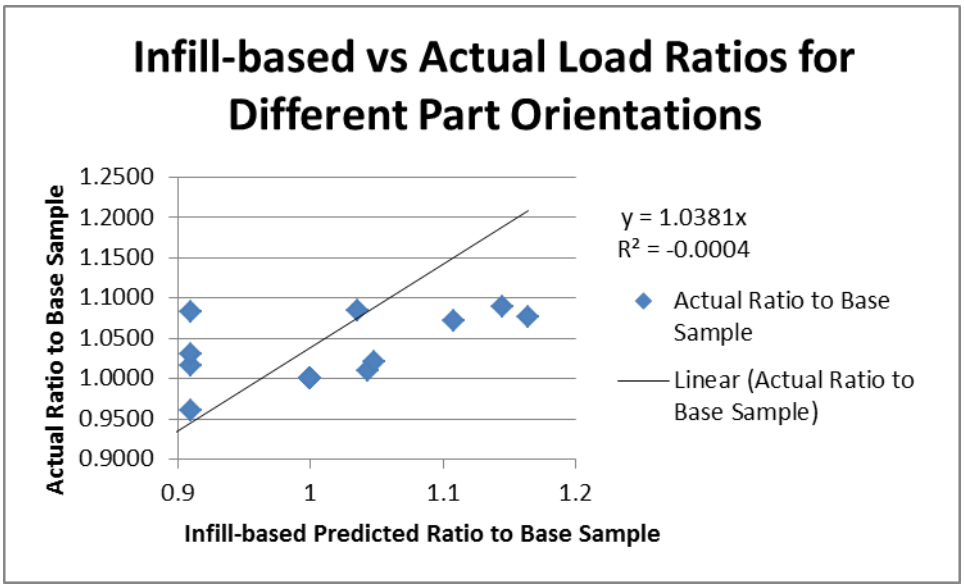

Figure 25: Lower Bound vs Actual Load Ratios for Different Part Orientations

The infill analysis was similarly inaccurate, with an R^2 value of -0.0004, showing little to no correlation. There was a peak error of -26%, with an average error of -8% and an average absolute error of 10%. However, these errors are even more significant in this case, since the largest actual ratio was 1.21. The error is greater than the changes in the model.

Because the lower bound model does not use the infill percentage as a variable, its usefulness for comparative analysis was not analyzed.

3.1.3 Infill-based Analysis

The infill-based model had accurate results overall. This model linearly interpolates between the upper and lower bound strengths based on the percentage of infill in the model.

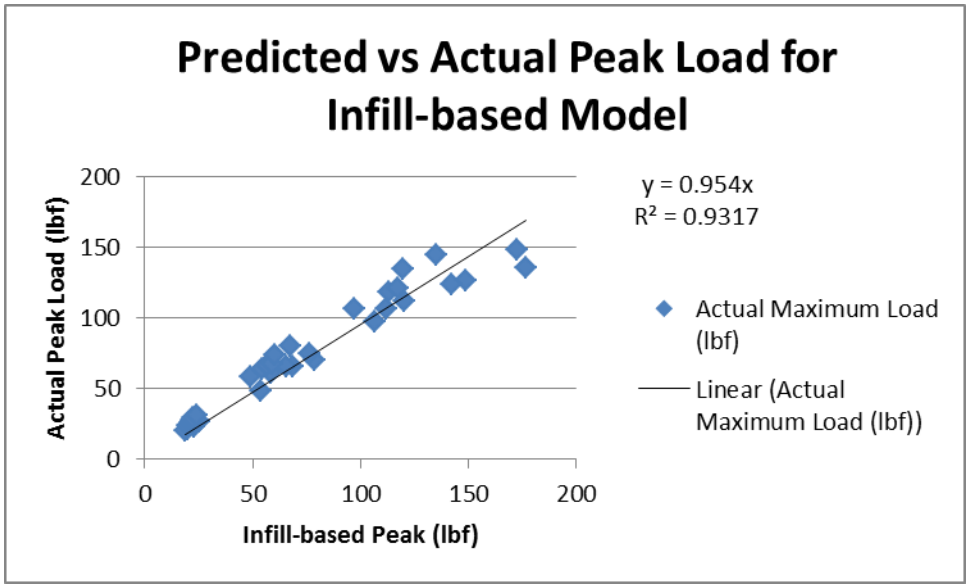

Figure 26: Predicted vs Actual Peak Load for Infill-based Model

As shown in Figure 26, the infill-based model is very accurate, with less than 5% RMS error and R^2=0.9317. This is the best of all models considered.

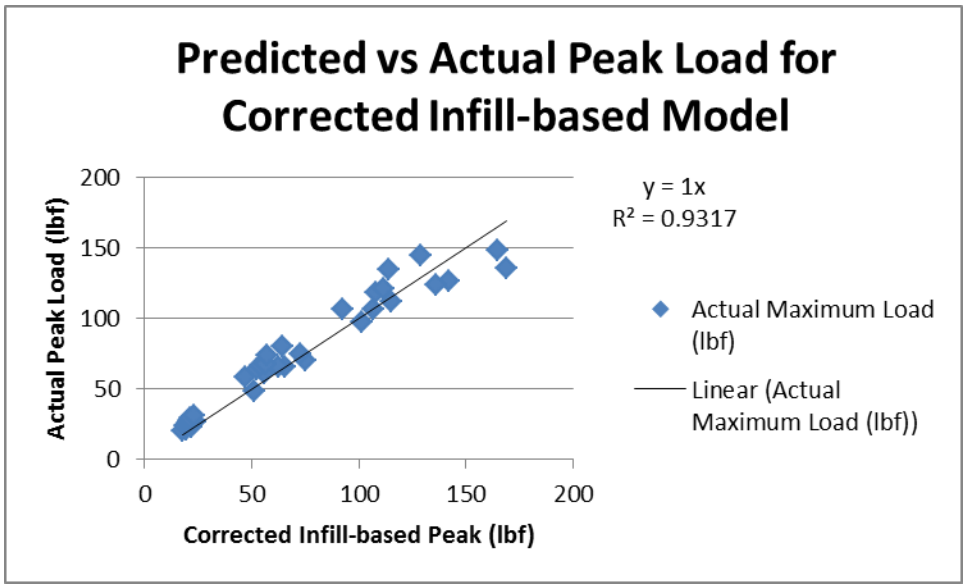

Figure 27: Predicted vs Actual Peak Load for Corrected Infill-based Model

Figure 27 shows the results from this compensated model, which minimizes the RMS error and the maximum discrepancy. While there is inaccuracy, predicted values are still quite close to absolute.

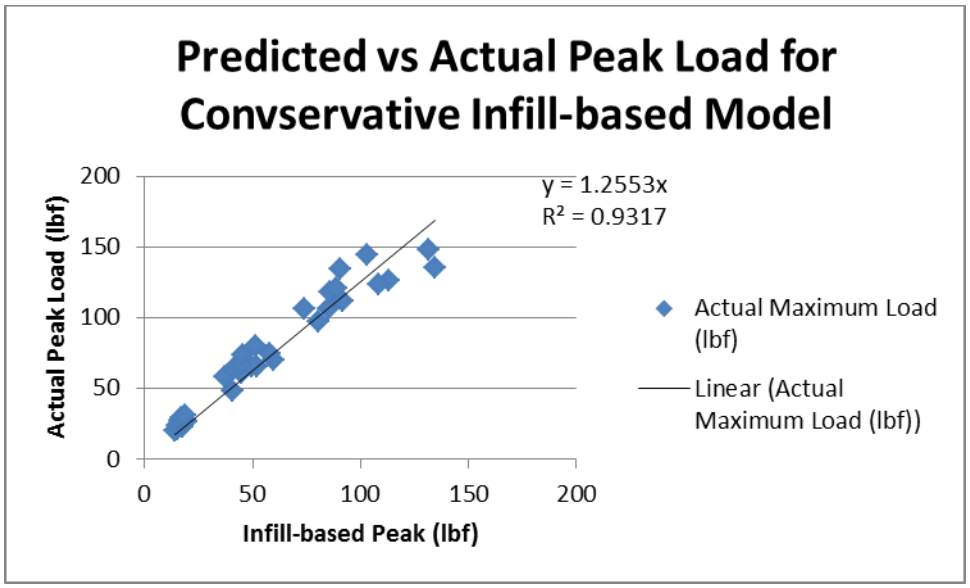

Figure 28: Predicted vs Actual Peak Load for Conservative Infill-based Model

Figure 28 shows the model after it has been corrected to provide conservative data. The model was adjusted until all predictions were lower than the actual breaking load. This has high average error of 27%, and peak error of 41%, but should always give conservative results.

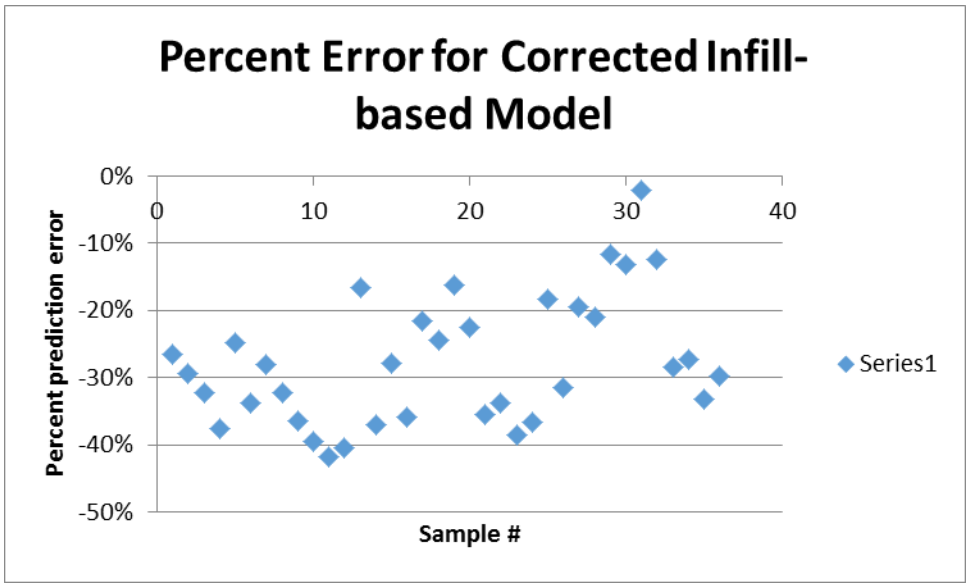

Figure 29: Percent Error for Corrected Infill-based Model

Figure 29 shows the percent error for the corrected infill-based model. The peak error is 26%, with -8% average error and 12% average absolute error. Again, this is the best of all of the models tested.

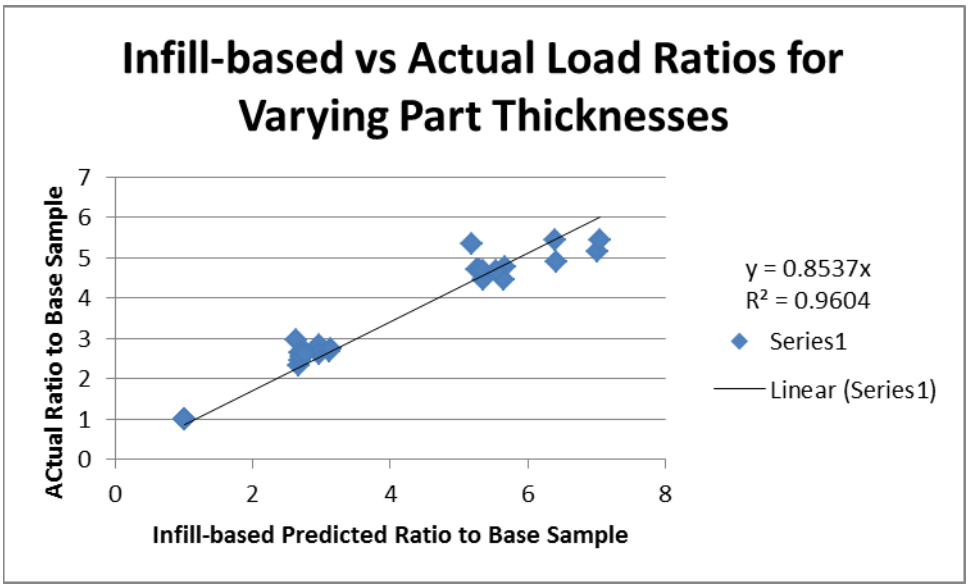

Figure 30: Infill-based vs Actual Load Ratios for Varying Part Thicknesses

The infill-based model was less accurate than the lower bound for comparative analysis of varying part thicknesses, as shown in Figure 30. There was 13% average error and 14% average absolute error. There was a peak error of 36%. It generally over-estimates the effect of changing part sizes, though not as much as the upper bound estimate.

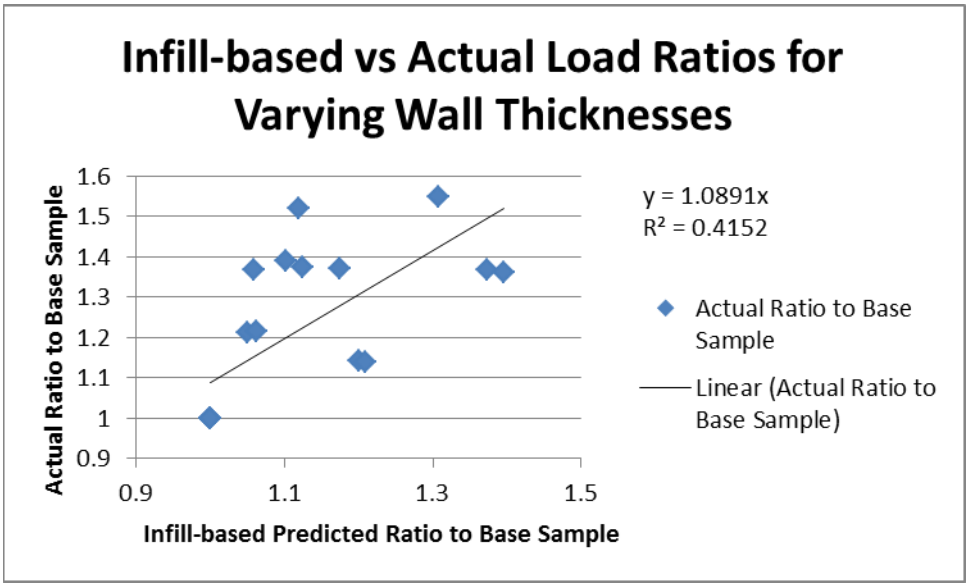

Figure 31: Infill-based vs Actual Load Ratios for Varying Wall Thicknesses

The results from wall thickness variation, in Figure 31, were similar to those for lower bound estimates. This is not surprising, as the areas of the equation that deal with wall thickness are very similar. There was a maximum error of -26%, an average error of -11%, and average absolute error of 13%.

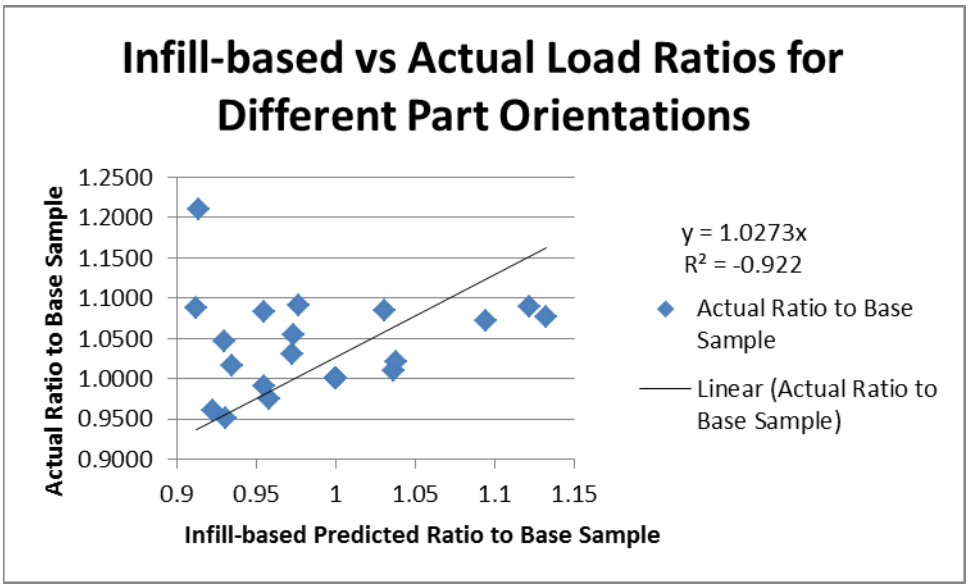

Figure 32: Infill-based vs Actual Load Ratios for Different Part Orientations

Figure 32 shows the predicted vs actual load ratios for the different part orientations. While there were outliers, as a whole the data conforms well to theory. There is a peak error of 24%, with an average error of -5% and an average absolute error of 7%. This is quite accurate.

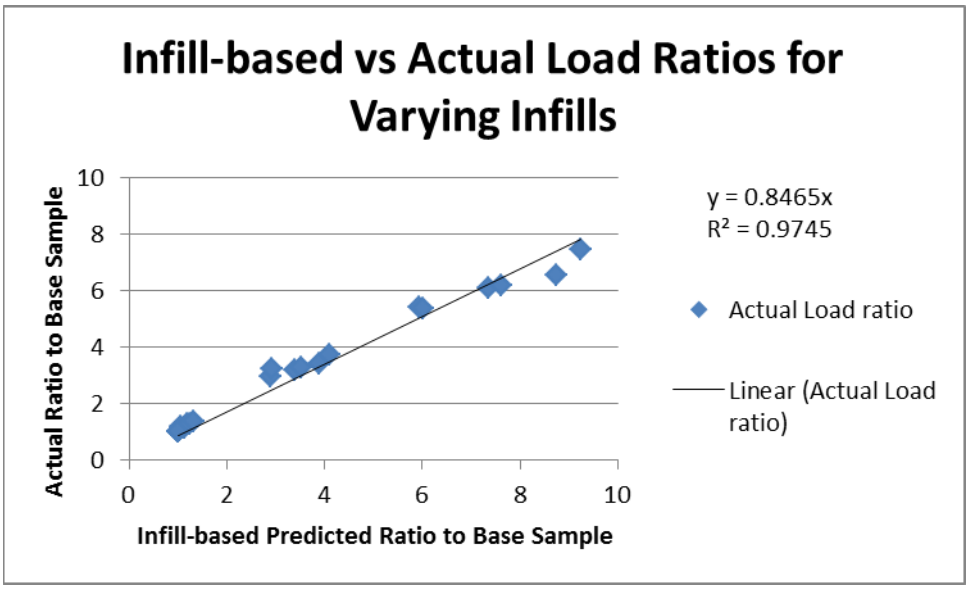

Figure 33: Infill-based vs Actual Load Ratios for Varying Infill Percentages

As shown in Figure 33, there is fairly significant error for comparisons of infill strength of roughly 15% RMS. The model tends to over predict the effect of infill on part strength. However, it is still fairly close, with an average error of 7% and an average absolute error of 11%. The peak error is 33%.

3.2 Truss Testing Fixture

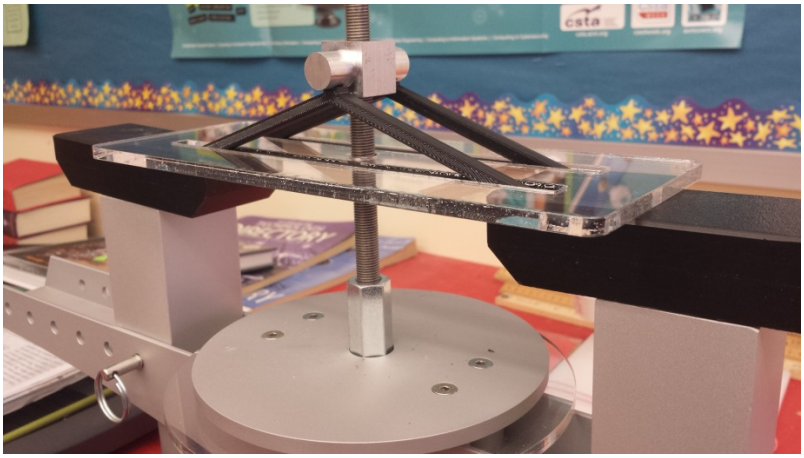

Figure 34: Truss bridge testing fixture

The fixture for analyzing trusses was overall successful, breaking all of the bridges tested. A picture of the setup in use can be found in Figure 34. However, several issues still developed during testing.

1. The acrylic loading plate initially was too tight-fitting around the parts. As load was placed, the bridges pressed against the insides of the slots. This makes results inaccurate, and also poses a minor safety hazard by potentially breaking the acrylic loading plate. This problem was resolved by increasing the size of the slots.
2. Some of the example parts were not symmetric, and didn't fit into the acrylic loading plate. This problem was caused by poor communication of the exact design requirements. It was resolved by removing the plate for those tests, since it is only intended to speed part alignment in setup and isn't necessary for actual testing.
3. Printing time was still higher than optimal, caused by the need for two separate bridges to be tested. This problem was not resolved during the course of the project.

Despite these issues, the fixture was successful in facilitating the experiments. More information on the results of the truss bridges can be found in the IQP group's report (Chamberlain & Meyers, 2016).

4.0 Discussion

This section interprets the results from the project, provides suggestions for how they can be used, and discusses avenues for further research.

4.1 Beam Analysis

Of the three models tested, the infill-based model is the most accurate, with the line of best fit agreeing to within 5% of theoretical. It is concluded that with an appropriate safety factor applied, the infill based model can provide safe and reasonably accurate estimates for part strength. The following equation for I_x is therefore proposed: $I_{x\,infill} = k\left(\frac{bh^3}{12} - (1 - \%I)\frac{(b-2w_t)(h-2c_t)^3}{12}\right)$, where $k = 1.05$ for the line of best fit and $k = 0.76$ for conservative analysis.

For comparative analysis, it was suitable for wall thickness and part orientation, with a roughly 1:1 slope. However, it was much less accurate for analyzing infill and outside part dimensions, over predicting their effects by nearly 20%. Caution is recommended, since this can lead to overestimating part strength.

The lower bound analysis had overall slightly lower accuracy. It consistently generated lower predictions for part strength. This could be useful for conservative design estimates, but the properly compensated infill-based model is more accurate for that function as well. The lower bound model is reasonably accurate in most circumstances, but is almost universally less accurate than the infill-based model for similar equation complexity, and therefore has little recommend it over that model.

The one area, however, where it excels is in comparative analysis of part dimensions, where it has a more accurate fit than the infill-based model. This was surprising, since the equations are quite similar. It is therefore recommended for estimating changes in part strength as thickness and width change.

The upper bound model did a poor job overall of predicting part failure. It consistently overestimated part strength, and had significant inaccuracy in comparative analysis as well. However, it has relatively low equation complexity, and may be useful for rough order-of-magnitude calculations, or for applications with particularly large factors of safety.

4.2 Bridge Testing Fixture

The device that was used was ultimately successful, and proves the validity of using 3d printed bridges as an introductory truss project. Out of the challenges that were encountered, all but one were easily solved without needing significant design changes. However, the last challenge, excessive printing time, is unavoidable with the two bridge design.

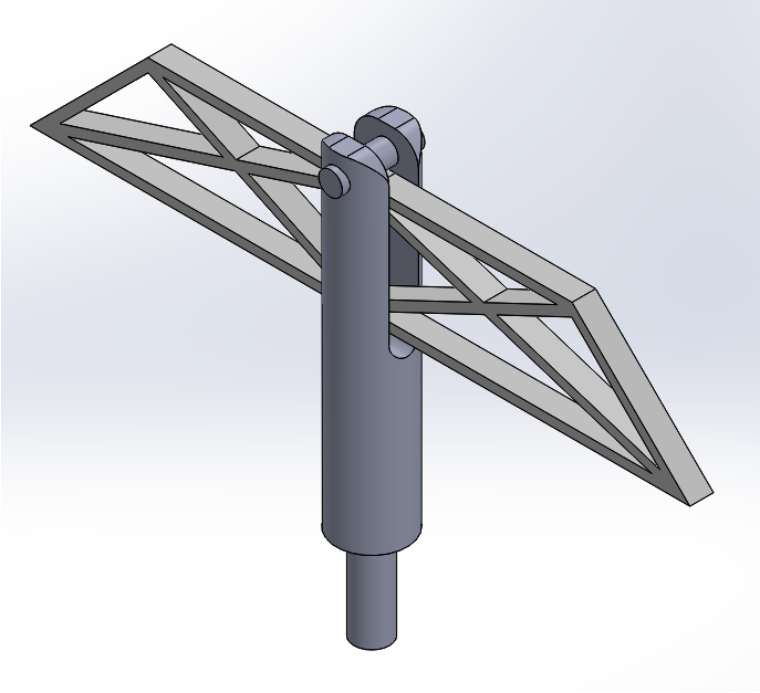

Figure 35: Proposed Truss Bridge Testing Device

A quick mockup of a proposed replacement design is pictured in Figure 35. Rather than threading onto the existing rod like the previous design did, this version replaces it entirely. The bottom section is threaded to install in place of the rod; this could be replaced with a different attachment system to match any specific testing device. The bridge is inserted through a vertical slot in the testing device, and a pin then applies the load down onto the bar. A shoulder bolt may be a good substitute for a straight pin, since it can be easily removed later if necessary, and won't risk bending the walls when installed.

There are several downsides to this approach, however. First, this design is less flexible in terms of what bridges it can break. The height and depth of the slot limit the bridge dimensions, while the length of the threaded portion needs to be carefully matched to the testing machine. Also, this design is more complicated to manufacture, with a deep slot, and an external thread that needs to be cut on a lathe or with a threading die. However, it resolves entirely the issue of requiring multiple bridges to be printed, a definite advantage over the previous method. The external thread could, if necessary, be replaced with a threaded rod tapped into the main body.

It is clear that existing testing devices can be easily adapted to test 3d printed bridges. However, the techniques proposed here may not function for all testing devices, since their designs could vary significantly. It is important to carefully analyze every setup and design not just the device but also the bridges to suit its capabilities.

4.3 Future Research

The outlier data points in the beam analysis were generally attributed more to variability in the 3d printing process than to inaccuracies in the model. This is supported by the symmetry of the errors in most cases, which suggests that the trend does follow the model overall. However, more testing is

necessary to experimentally verify how much of the inaccuracy was due to part variations and how much is due to the equations.

The areas where the errors were not symmetrical were the infill percentage and the outside dimensions of the part. Research should focus on more detailed analysis to better predict their effects on part behavior.

Lastly, the accuracy of the proposed models in more complex situations should be evaluated, such as cantilevered beams under complex loads, or using different materials and printing settings. Further research on adapting truss bridge models to better describe 3d printed parts would also be useful.

5.0 Conclusions

This project evaluated the accuracy of traditional engineering equations for two classic problems: truss bridges and beams in bending. Effective methods for testing these models were developed and utilized to analyze how well the equations describe FDM 3d printed parts. Specific strengths and weaknesses of theoretical models were described, and suggestions for future use have been given.

- Simple modifications to existing structure testing devices can make them suitable for 3d printed bridges.
- The proposed infill-based model for beam strength can accurately predict beam failure in direct analysis.
- The infill-based model is accurate for direct comparison of wall thickness and orientation. However, it is less accurate for infill and part dimensions, over-predicting their effects on part strength.
- Lower bound estimates of beam strength are only preferable over infill-based estimates when doing comparative analysis of the outside part dimensions.
- Upper bound estimates of beam strength are not generally useful for either direct or comparative analysis. They may be useful for either order-of-magnitude analysis or applications where significant inaccuracy is acceptable.
- Further research should focus on analyzing the effects of infill and outside part dimensions on beam strength, and on evaluating the model's accuracy in more complex situations.

6.0 References

3D design tips. (2014, February 4). Retrieved from Ultimaker: http://wiki.ultimaker.com/3D_design_tips

Additive Manufacturing. (2016). Retrieved from Additive Manufacturing: http://www.additivemanufacturing.media/

Ahn, S.-H., Montero, M., Odell, D., Roundy, S., & Wright, P. K. (2002). Anisotropic material properties of fused deposition modeling ABS. *Rapid Prototyping Journal*, 248-257.

ASTM International. (2016). *D790-15: Standard Test Methods for Flexural Properties of Unreinforced and Reinforced Plastics and Electrical Insulating Materials.*

Barrentine, L. B. (2014). *Introduction to Design of Experiments : A Simplified Approach.* ASQ Quality Press.

Chamberlain, S., & Meyers, M. (2016). *Incorporation of 3d Printing in STEM Curricula.* Worcester Polytechnic Institute.

Dumas, J., Hergel, J., & Lefebvre, S. (2014). Bridging the gap: automated steady scaffoldings for 3D printing. *ACM Transactions on Graphics (TOG) - Proceedings of ACM SIGGRAPH 2014, 33*(4).

Encyclopaedia Britannica. (2016). *bridge*. Retrieved from Encyclopaedia Britannica Online: http://www.britannica.com/technology/bridge-engineering

Franky. (2014, April 17). *3D Printing Tips & Tricks – How to 3D Model A Great 3D Print*. Retrieved from i.materialise: https://i.materialise.com/blog/tips-and-tricks-to-design-3d-printable-models

Hultgren, K. (2013, December 11). *Top Ten Tips: Designing Models For 3D Printing*. Retrieved from Make: http://makezine.com/2013/12/11/top-ten-tips-designing-models-for-3d-printing/

Kesner, S., & Howe, R. (2011). Design Principles for Rapid Prototyping Forces. *IEEE/ASME TRANSACTIONS ON MECHATRONICS, 16*(5).

Klahn, C., Leutenecker, B., & Meboldt, M. (2014). Design for Additive Manufacturing – Supporting the Substitution of. *Procedia CIRP, 21*, 138-143.

Norton. (2014). *Machine Design: An Integrated Approach, Fifth Edition.* Worcester: Prentice Hall.

Pitsco Education. (2016). *Structures Testing Instrument*. Retrieved from Pitsco Education: http://www.pitsco.com/Structures_Testing_Instrument

Sayre, R. (2014). *A Comparative Finite Element Stress Analysis of Isotropic and Fusion Deposited 3D Printed Polymer.* Rensselaer Polytechnic Institute.

Sculpteo. (n.d.). *Design Guidelines for 3d Printing: Our Tips for Preparing a Perfect 3d Model.*

Shapeways. (2015). *3d Printing and Design Tutorials*. Retrieved from Shapeways: http://www.shapeways.com/tutorials/?li=bc

Smythe, C. (2015). *Functional Design for 3D Printing 2nd edition: Designing 3D printed things for everyday use.* CreateSpace Independent Publishing Platform.

Stava, O., Vanek, J., Benes, B., Carr, N. A., & Mvech, R. (2012). Stress Relief: Improving Structural Strength of 3D Printable Objects. *ACM Transactions on Graphics, 31*(4), 1-11.

Tracy, Novak, J., & Cline, L. (n.d.). *The 3D Printing Design Guide*. Retrieved from Pinshape: https://pinshape.com/3d-printing-design-guide

Umetani, N., & Schmidt, R. (2013). Cross-sectional structural analysis for 3d printing optimization. *SIGGRAPH Asia*, 5.

www.3ders.org. (n.d.). *3D Printing Basics*. Retrieved from www.3ders.org: http://www.3ders.org/3d-printing-basics.html

Zhang, X., Xia, Y., Wang, J., Yang, Z., Tu, C., & Wang, W. (2015). Medial axis tree—an internal supporting structure for 3D printing. *Computer Aided Geometric Design, 35-36*, 149-162.

7.0 Appendices

7.1 Full List of Academic Research

This list is not a complete list of every source available in academic literature on 3d printing design. However, it does provide a representative sample.

Adam, G. A., & Zimmer, D. (2014). Design for Additive Manufacturing—Element transitions and aggregated structures. CIRP Journal of Manufacturing Science and Technology, 7, 20-28.

Ahn, S.-H., Montero, M., Odell, D., Roundy, S., & Wright, P. K. (2002). Anisotropic material properties of fused deposition modeling ABS. Rapid Prototyping Journal, 248-257.

Dumas, J., Hergel, J., & Lefebvre, S. (2014). Bridging the gap: automated steady scaffoldings for 3D printing. ACM Transactions on Graphics (TOG) - Proceedings of ACM SIGGRAPH 2014, 33(4).

Günther, D., Heymel, B., Günther, J. F., & Ederer, I. (2014). Continuous 3D-printing for additive manufacturing. Rapid Prototyping Journal, 20(4), 320-327.

Johnson, W., Rowell, M., Deason, B., & Eubanks, M. (2014). Comparative evaluation of an open-source FDM system. Rapid Prototyping Journal, 20(3), 205-214.

Kesner, S., & Howe, R. (2011). Design Principles for Rapid Prototyping Forces. IEEE/ASME TRANSACTIONS ON MECHATRONICS, 16(5).

Klahn, C., Leutenecker, B., & Meboldt, M. (2014). Design for Additive Manufacturing – Supporting the Substitution of. Procedia CIRP, 21, 138-143.

Lanzotti, A., Maria Del Guidice, D., Lepore, A., Staiano, G., & Martorelli, M. (2015). On the Geometric Accuracy of RepRap Open-Source Three-Dimensional Printer. Journal of Mechanical Design, 137.

Liu, S., Li, Q., Chen, Wenjiong, Tong, L., & Cheng, G. (2015). An identification method for enclosed voids restriction in manufacturability design for additive manufacturing structures. Frontiers of Mechanical Engineering, 10(2), 126-137.

Ma, R. R., Belter, J. T., & Dollar, A. M. (2015). Hybrid Deposition Manufacturing: Design Strategies for Multimaterial Mechanisms Via Three-Dimensional Printing and Material Deposition. Journal of Mechanisms and Robotics, 7.

Martínez, J., Diéguez, J., Ares, J., Pereira, A., & Pérez, J. (2012). Modelization and Structural Analysis of FDM Parts. AIP Conf. Proc., 1431, 842-848.

Meisel, N., & Williams, C. (2015). An Investigation of Key Design for Additive Manufacturing Constraints in Multi-Material 3D Printing. Journal of Mechanical Design.

Meisel, N., & Williams, C. (2015). Design and assessment of a 3D printing vending machine. Rapid Prototyping Journal, 21(5), 471-481.

Rosen, D. (2014). Design for Additive Manufacturing: Past, Present, and Future Directions. Journal of Mechanical Design, 136.

Sayre, R. (2014). A Comparative Finite Element Stress Analysis of Isotropic and Fusion Deposited 3D Printed Polymer. Rensselaer Polytechnic Institute.

Singh, R. (2013). Some investigations for small-sized product fabrication with FDM for plastic components. Rapid Prototyping Journal, 19(1), 58-63.

Singh, R. (2013). Some investigations for small-sized product fabrication with FDM for plastic components. Rapid Prototyping Journal, 19(1), 58-63.

Song, P., Fu, Z., Liu, L., & Fu, C.-W. (2015). Printing 3D objects with interlocking parts. Computer Aided Geometric Design, 35-36, 137-148.

Turner, B. N., Strong, R., & Gold, S. A. (2014). A review of melt extrusion additive manufacturing processes: I. Process design and modeling. Rapid Prototyping Journal, 20(3), 192-204.

Zhang, X., Xia, Y., Wang, J., Yang, Z., Tu, C., & Wang, W. (2015). Medial axis tree—an internal supporting structure for 3D printing. Computer Aided Geometric Design, 35-36, 149-162.

7.2 Full List of Non-academic Research

This list is not a complete list of every source available for the public on 3d printing design. However, it does provide a representative sample of the literature.

3D design tips. (2014, February 4). Retrieved from Ultimaker: http://wiki.ultimaker.com/3D_design_tips

Additive Manufacturing. (2016). Retrieved from Additive Manufacturing: http://www.additivemanufacturing.media/

Franky. (2014, April 17). 3D Printing Tips & Tricks – How to 3D Model A Great 3D Print. Retrieved from i.materialise: https://i.materialise.com/blog/tips-and-tricks-to-design-3d-printable-models

Hultgren, K. (2013, December 11). Top Ten Tips: Designing Models For 3D Printing. Retrieved from Make: http://makezine.com/2013/12/11/top-ten-tips-designing-models-for-3d-printing/

Sculpteo. (n.d.). Design Guidelines for 3d Printing: Our Tips for Preparing a Perfect 3d Model.

Shapeways. (2015). 3d Printing and Design Tutorials. Retrieved from Shapeways: http://www.shapeways.com/tutorials/?li=bc

Smythe, C. (2015). Functional Design for 3D Printing 2nd edition: Designing 3D printed things for everyday use. CreateSpace Independent Publishing Platform.

Stava, O., Vanek, J., Benes, B., Carr, N. A., & Mvech, R. (2012). Stress Relief: Improving Structural Strength of 3D Printable Objects. ACM Transactions on Graphics, 31(4), 1-11.

Tracy, Novak, J., & Cline, L. (n.d.). The 3D Printing Design Guide. Retrieved from Pinshape: https://pinshape.com/3d-printing-design-guide

Umetani, N., & Schmidt, R. (2013). Cross-sectional structural analysis for 3d printing optimization. SIGGRAPH Asia, 5.

www.3ders.org. (n.d.). 3D Printing Basics. Retrieved from www.3ders.org: http://www.3ders.org/3d-printing-basics.html

7.3 Detailed Drawings of Bridge Testing Device

7.3.1 First Generation of Device

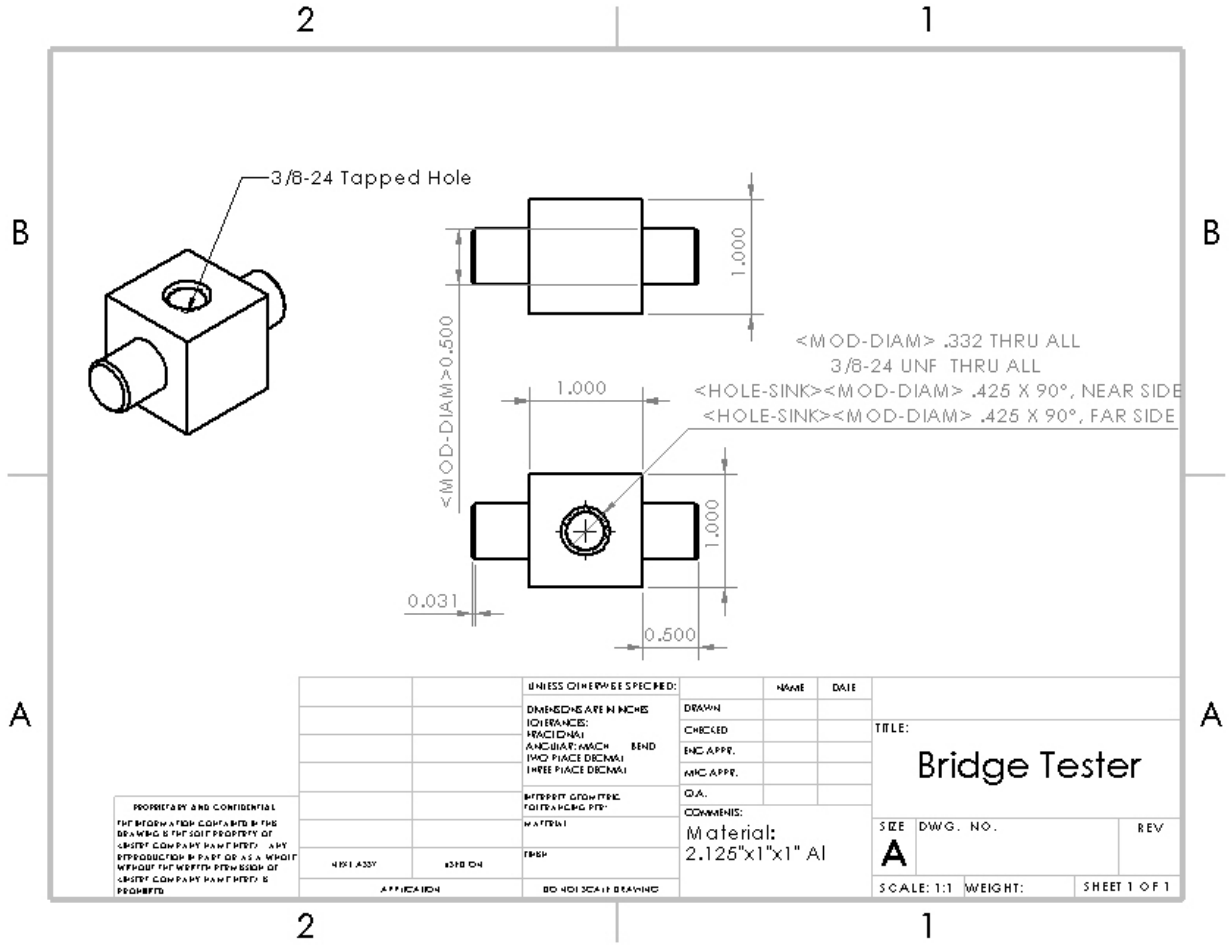

Figure 36: Drawing for First Version of Bridge Tester

7.3.2 Second Generation of Device

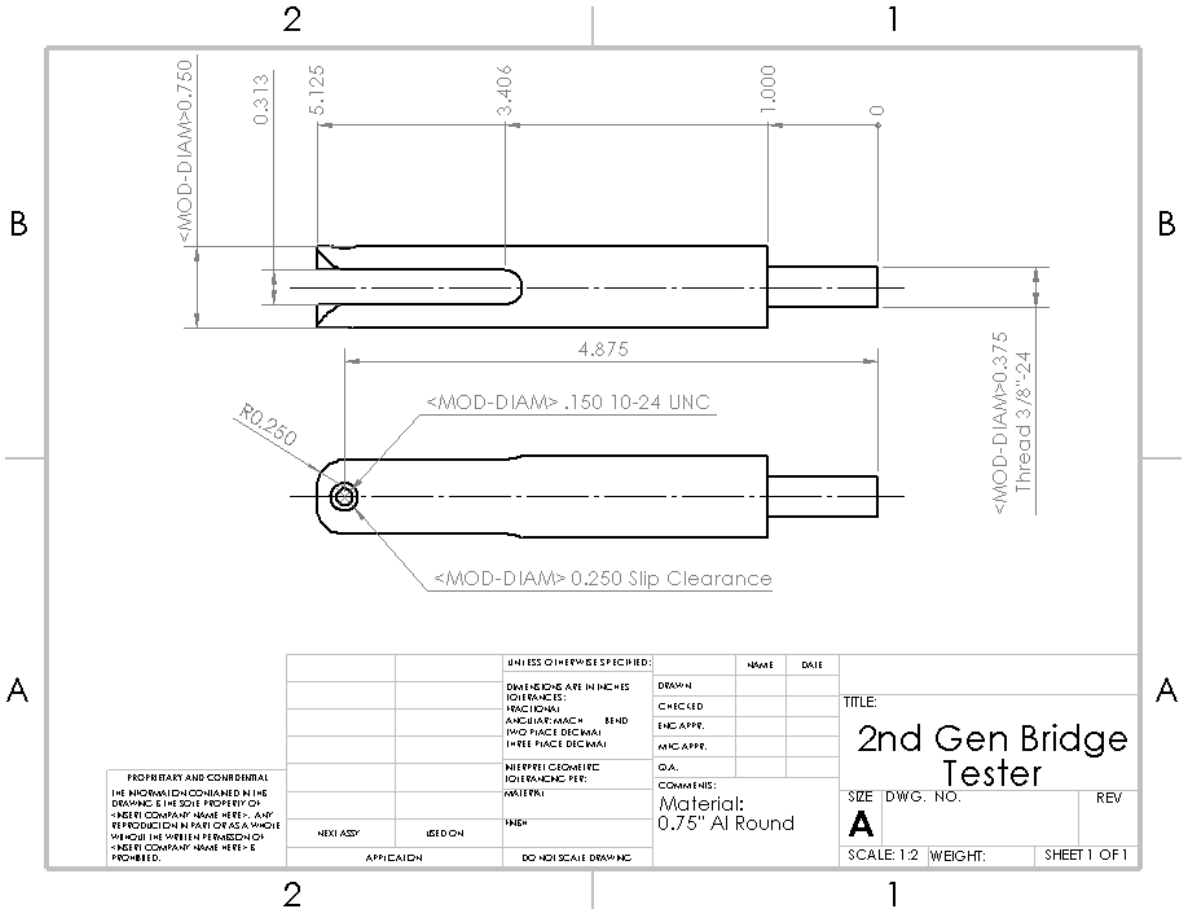

Figure 37: Drawing for Second Version of Bridge Tester

A 10-24 shoulder screw with a ¼", 0.625" long shoulder goes through the slot and serves as the load applicator.

7.4 Full 3d Printing Parameters

Table 1: Full 3d Printing Parameters

Item	Value
Extruder Temperature	230 C
Platform Temperature	110 C
Travel Speed	150 mm/s
Z-axis Travel Speed	23 mm/s
Minimum Layer Duration	5.0 s
Filament Cooling Fan Speed	0.50
Bridge Print Speed	40 mm/s
First Layer Print Speed	30 mm/s
First Layer Raft Print Speed	50 mm/s
Floor Surface Fill Print Speed	90 mm/s
Infill Print Speed	90 mm/s
Insets Print Speed	90 mm/s
Outline Print Speed	40 mm/s
Raft Print Speed	90 mm/s
Raft Base Print Speed	10 mm/s
Roof Surface Fills	90 mm/s
Sparse Roof Surface Fills	90 mm/s
Infill Layer Height	0.20 mm
Infill Pattern	Hexagonal
Layer Height	0.20 mm
Roof Thickness	0.80 mm
Floor Thickness	0.80 mm
Coarseness	0.00010 mm
Fixed Shell Starting Point	215 degrees
Filament Diameter	1.77 mm
Retraction Distance	1.3 mm
Retraction Speed	25 mm/s
Restart Speed	25 mm/s
Extra Restart Distance	0.0 mm
Extra Restart Speed	25 mm/s

7.5 Detailed Derivation of Beam Strength Predictions

The equation for F_{max} is based on the maximum tensile stress for a beam in bending and the moment that beam experiences (Norton, 2014).

$\sigma_{max}(M) = Mh/2I_x$

$M(F) = \frac{FL}{4} \Rightarrow \sigma_{max}(F) = \frac{FLh}{8I_x}$

$\sigma_{max} = \sigma_b \Rightarrow F_{max} = \frac{8I_x\sigma_b}{lh}$

$F_{max} = \frac{4I_x\sigma_b}{lh/2}$

The moment area of inertia calculations are from standard engineering equations for rectangular beams (Norton, 2014).

The upper bound calculation assumes that the beams is a solid bar, and thus uses the traditional equation, $I_x = \frac{bh^3}{12}$. The lower bound equation assumes that the beam is entirely hollow, with given wall and ceiling thicknesses. The I_x for the internal area of the beam is therefore subtracted from the upper bound calculation, giving $I_x = \frac{bh^3}{12} - \frac{(b-2w_t)(h-2c_t)^3}{12}$. Lastly, the infill-based model linearly interpolates between these two, based on the percent infill $\%I$, which results in $, I_x = \frac{bh^3}{12} - (1 - \%I)\frac{(b-2w_t)(h-2c_t)^3}{12}$.

7.6 Specimen Coding Nomenclature

All specimens were labelled with a standardized four digit code. The first digit referred to the orientation of the part. The second digit was the infill percentage. The third was the outside size of the specimen. The fourth digit was the wall thickness. See the below table for the specific dimensions coded by each digit.

Table 2: Specimen Orientation Code

Orientation Code	Orientation
1	Printing axis vertical
2	Printing axis horizontal

Table 3: Specimen Infill Code

Infill Code	Infill Percentage
1	10%
2	20%
3	40%
4	60%

Table 4: Specimen Size Code

Size Code	Outside Part Dimensions
1	0.25”
2	0.375”
3	0.5”

Table 5: Specimen Wall Code

Wall Code	Wall Thickness
1	1 layer
2	2 layers
3	3 layers
4	4 layers

7.7 Predicted Beam Data

Below are the theoretical predictions for peak beam load using each of the theoretical calculations. See 7.6 Specimen Coding Nomenclature for information on the label and variable numbering.

Table 6: Predicted Bar Data

Specimen Label	I Full Bar	I Empty Area	I Shell	Upper breaking limit	Lower Breaking Limit	Infill-based Breaking Point
	(in^4)	(in^4)	(in^4)	(lbf)	(lbf)	(lbf)
1111	0.000326	0.000111	0.000215	29.166667	19.265646	15.394369
2111	0.000326	0.000130	0.000196	29.166667	17.527894	14.205746
1121	0.000326	0.000111	0.000215	29.166667	19.265646	16.146846
2121	0.000326	0.000130	0.000196	29.166667	17.527894	15.090293
1131	0.000326	0.000111	0.000215	29.166667	19.265646	17.651801
2131	0.000326	0.000130	0.000196	29.166667	17.527894	16.859386
1141	0.000326	0.000111	0.000215	29.166667	19.265646	19.156756
2141	0.000326	0.000130	0.000196	29.166667	17.527894	18.628480
1112	0.000326	0.000098	0.000228	29.166667	20.419163	16.183374
2112	0.000326	0.000090	0.000236	29.166667	21.140287	16.676623
1113	0.000326	0.000085	0.000241	29.166667	21.572680	16.972380
2113	0.000326	0.000059	0.000267	29.166667	23.915246	18.574695
1211	0.001648	0.000830	0.000818	98.437500	48.883046	40.917254
2211	0.001648	0.000915	0.000732	98.437500	43.754462	37.409302
1221	0.001648	0.000830	0.000818	98.437500	48.883046	44.683392
2221	0.001648	0.000915	0.000732	98.437500	43.754462	41.565213
1231	0.001648	0.000830	0.000818	98.437500	48.883046	52.215669
2231	0.001648	0.000915	0.000732	98.437500	43.754462	49.877035
1241	0.001648	0.000830	0.000818	98.437500	48.883046	59.747946
2241	0.001648	0.000915	0.000732	98.437500	43.754462	58.188856
1212	0.001648	0.000770	0.000878	98.437500	52.454538	43.360154
2212	0.001648	0.000731	0.000917	98.437500	54.746159	44.927623
1213	0.001648	0.000710	0.000938	98.437500	56.026031	45.803055
2213	0.001648	0.000574	0.001074	98.437500	64.156418	51.364240
1311	0.005208	0.003149	0.002059	233.333333	92.265278	80.842784
2311	0.005208	0.003380	0.001828	233.333333	81.915021	73.763208
1321	0.005208	0.003149	0.002059	233.333333	92.265278	91.563956
2321	0.005208	0.003380	0.001828	233.333333	81.915021	85.270999
1331	0.005208	0.003149	0.002059	233.333333	92.265278	113.006300
2331	0.005208	0.003380	0.001828	233.333333	81.915021	108.286583
1341	0.005208	0.003149	0.002059	233.333333	92.265278	134.448645
2341	0.005208	0.003380	0.001828	233.333333	81.915021	131.302166
1312	0.005208	0.002985	0.002224	233.333333	99.625351	85.877073

2312	0.005208	0.002878	0.002330	233.333333	104.400248	89.143103
1313	0.005208	0.002820	0.002388	233.333333	106.985423	90.911363
2313	0.005208	0.002428	0.002780	233.333333	124.541435	102.919675

7.8 Raw Data from Beam Testing

Below are the experimental peak beam loads. See 7.6 Specimen Coding Nomenclature for information on the label and variable numbering.

Table 7: Raw Data from Beam Testing

#	Specimen Label	Specimen Orientation	Specimen Size	Specimen Infill	Specimen Wall Thickness	Maximum Load (N)
1	1111	1	1	1	1	92.09
2	2111	2	1	1	1	88.45
3	1121	1	1	2	1	104.5
4	2121	2	1	2	1	106.17
5	1131	1	1	3	1	103.03
6	2131	2	1	3	1	111.63
7	1141	1	1	4	1	116.97
8	2141	2	1	4	1	120.58
9	1112	1	1	1	2	111.73
10	2112	2	1	1	2	121.16
11	1113	1	1	1	3	127.87
12	2113	2	1	1	3	137.14
13	1211	1	2	1	1	215.42
14	2211	2	2	1	1	260.81
15	1221	1	2	2	1	272.02
16	2221	2	2	2	1	284.7
17	1231	1	2	3	1	292.58
18	2231	2	2	3	1	289.77
19	1241	1	2	4	1	313.07
20	2241	2	2	4	1	329.89
21	1212	1	2	1	2	294.84
22	2212	2	2	1	2	297.55
23	1213	1	2	1	3	327.41
24	2212	2	2	1	3	356.47
25	1311	1	3	1	1	434.07
26	2311	2	3	1	1	472.11
27	1321	1	3	2	1	499.1
28	2321	2	3	2	1	474.31
29	1331	1	3	3	1	561.86

30	2331	2	3	3	1	548.06
31	1341	1	3	4	1	602.79
32	2341	2	3	4	1	657.54
33	1312	1	3	1	2	526.9
34	2312	2	3	1	2	538.18
35	1313	1	3	1	3	596.81
36	2313	2	3	1	3	642.79